The Eidsfjord anorthosite, Vesterålen, Norway: field observations and geochemical data

GREGOR MARKL

Markl, G. 1998: The Eidsfjord anorthosite, Vesterålen, Norway: field observations and geochemical data. *Norges geologiske undersøkelse Bulletin 434, 53-75*

New fieldwork in the Eidsfjord anorthosite on Langøy, Vesterålen, Nordland, has revealed that the anorthosite in the centre of the investigated complex is associated with large amounts of monzonitic and more mafic rocks which span the compositional range between norite, gabbronorite and ferrodiorite. The ferrodiorites occur as bodies and dykes within and at the margins of the anorthosite and in the country rocks. Many of these mafic rocks are fine-grained and are believed to reflect liquid compositions. Some of them clearly postdate the anorthosite, whereas others appear to be contemporaneous with it.

Chemical compositions of the rocks in the Eidsfjord anorthosite, if plotted against $X_{Fe}^{whole\ rock}$, follow a trend from more primitive, Ca- and Al-rich gabbroic and noritic rocks towards the more Fe-, Ti-, P- and K-rich ferrodiorites and finally towards the Si- and K-rich monzonites which may reflect a fractionation trend. In terms of their X_{Fe}, the anorthositic rocks - which are cumulates and as such not directly comparable - fall between the gabbros/norites and the ferrodiorites. Mineralogically, this trend is also reflected by changes in the compositions of feldspars and pyroxenes: the most primitive rocks show plagioclase with $An_{>60}$, the anorthosites, gabbros and norites fall into the range An_{40}-An_{60}, the ferrodioritic rocks contain a strongly ternary plagioclase or a mesoperthitic alkali feldspar, and the monzonitic rocks contain a relatively Ca-poor alkali feldspar. Mafic minerals progressively become more Fe-rich. The typical mafic assemblage in all rock types is Cpx+Opx+Mt+Ilm (rarely only Ilm or Mt), the assemblage Cpx+Ol is uncommon, and only in one case has the assemblage Cpx+Opx+Pig been observed. Apatite in all rock types is very F-rich and contains appreciable amounts of Cl, but is generaly OH-free, pointing to the extremely dry nature of the melts that is also reflected by the anhydrous mineral assemblages. F and Cl in apatite vary systematically with X_{Fe} and may monitor the halogen contents of the melts during fractionation. Phase petrology indicates that the rocks intruded to mid-crustal levels of about 5 kbar at temperatures between 1000 and 1200 °C and an oxygen fugacity corresponding approximately to the FMQ-buffer (± 0.8 log units).

Field and geochemical data indicate that the Eidsfjord anorthosite may be regarded as a cumulate from a primitive, broadly basaltic magma and that the residual liquids of the anorthositic cumulates are ferrodiorites which further evolve to monzonites. The Eidsfjord anorthosite comprises a greater proportion of the related mafic rock types and exhibits slightly different phase assemblages when compared to the spatially close Mid-Proterozoic Flakstadøy anorthosite (FBC) on Lofoten, but the evolutionary trend is in agreement with the one proposed for the FBC.

Gregor Markl, Institut für Mineralogie, Petrologie und Geochemie, Albert-Ludwigs-Universität, Albertstrasse 23 b, D-79104 Freiburg, Germany. e-mail: markl@ruf.uni-freiburg.de

Introduction and geological setting

The anorthosite problem

Proterozoic massif-type anorthosites are still enigmatic rocks in spite of numerous efforts and some advances in the last 10-15 years to understand their petrogenesis (see Ashwal 1993, and references therein). The enigmatic facts are the huge size of the bodies which consist of more than 90 % plagioclase of almost homogeneous, intermediate composition (An_{40}-An_{60}, e. g. Morse 1981, Duchesne 1984, Ashwal 1993); the lack of any large amounts of associated mafic or ultramafic cumulates complementary to the anorthosites, and the lack of gravity anomalies which could imply that this material resides at depth; and the observation that, with only one younger exception (Gruber anorthosite in Antarctica, Markl et al. submitted), these rocks are confined to a period in the Earth´s history between about 900 and 1800 Ma (Ashwal 1993). It is now generally agreed that a two-stage model of formation best explains the observed features of anorthosites. According to this model, which was proposed by Emslie (1978) and many subsequent workers (e. g. Fram & Longhi 1992, Wiebe 1992, Longhi et al. 1993) plagioclase cumulates float on basic magma at the crust-mantle boundary while contemporaneously pyroxenes (and spinel?) fractionate and sink back into the mantle. The nature of the parent magma is still under debate, but based on field observations and geochemical arguments, Emslie (1989), Mitchell et al. (1995) and Markl & Frost (in press) have argued that it is of tholeiitic to high-Al basaltic composition, whereas Olson & Morse (1990) proposed an Fe- and Al-rich basaltic composition while Duchesne (1984) and Vander Auwera et al. (1998) argued for a monzonoritic parental magma composition. The plagioclase cumulates are buoyant and rise as crystal-rich mushes to mid-crustal levels where they finally solidify (e. g. Lafrance et al. 1996). This process of polybaric crystallization is supported by the finding of high-Al orthopyroxene megacrysts in many anorthosites (e. g. Emslie 1975, Longhi et al., 1993) that are interpreted to have formed under high pressures (about 15 kbar), and based on the phase petrology of the mafic assemblages it was

shown to work in the Flakstadøy anorthosite on the Lofoten Islands (Markl et al. i1998). The intruding anorthosite mushes contain significant amounts of interstitial, residual liquid and e. g. Mitchell et al. (1996) and Markl & Frost (in press) have proposed that this interstitial liquid is represented by the ferrodioritic rocks found in many Proterozoic anorthosite complexes. As the relative amounts of ferrodiorites to anorthosites in virtually all Proterozoic anorthosites are too small to support such a conclusion, Scoates et al. (1996) and Markl & Frost (submitted) proposed - based on isotopic data - that the ferrodiorites evolve by fractionation and assimilation of crustal material (e. g. anatectic melts from the host rocks) towards mangeritic and charnockitic rocks that are commonly observed in variable, but typically large amounts in association with Proterozoic anorthosites (e. g. Fuhrman et al. 1988, Kolker & Lindsley 1989, Emslie & Hunt 1990, Kolker et al. 1990, Emslie 1991, Duchesne & Wilmart 1997).

Regional geology

The island group of Lofoten-Vesterålen in Nordland, Norway, is composed of Archaean to Mid-Proterozoic basement gneisses into which gabbroic, anorthositic, mangeritic and charnockitic magmatic rocks intruded during Mid-Proterozoic time (1.8-1.7 Ga, Griffin et al. 1978, Malm & Ormaasen 1978, Wade 1985, Markl et al. 1998) (Fig. 1). A granulite-facies metamorphism at about 1.8 Ga has been recorded in many areas (e. g. Krogh 1977, Griffin et al. 1978, Olsen 1978), although a subsequent eclogite-facies (Markl & Bucher 1997) and two periods of amphibolite-facies metamorphism (Griffin et al. 1978, Hames & Andresen 1996) overprinted the granulites and the anhydrous mineral assemblages in the intrusive rocks to a certain extent. Based on phase equilibria among pyroxenes and plagioclase combined with the QUIIF method of Frost & Lindsley (1992) and Lindsley & Frost (1992), the intrusive mangerites and charnockites were shown to have intruded at about 4 kbar and >925 to 850 °C, respectively, while the anorthosite on Flakstadøy records a polybaric crystallization history from 9 to about 4 kbars at 1180 to 1120 °C, implying that the anorthosites, mangerites and charnockites on Lofoten intruded to the same depth of about 12 km (Markl et al. 1998).

There are three Proterozoic anorthosite complexes on the Lofoten Islands (Fig. 1); the almost inaccessible Moskenesøy anorthosite, the large Flakstadøy anorthosite which is associated with gabbroic and troctolitic rocks (Flakstadøy Basic Complex, FBC, of Markl et al. 1998) and the Eidsfjord anorthosite complex on the island of Langøy which is about 11 by 2 km in extent and which comprises rocks of anorthositic, ferrodioritic, noritic and monzonitic composition. The island of Langøy was mapped by Heier (1960) who also presented some data on mineral and whole-rock chemistry as well as on the modal composition of the various rock types. For detailed descriptions of the basement rocks in the vicinity of the Langøy anorthosite the reader is therefore referred to Heier (1960). Priesemann (1982)

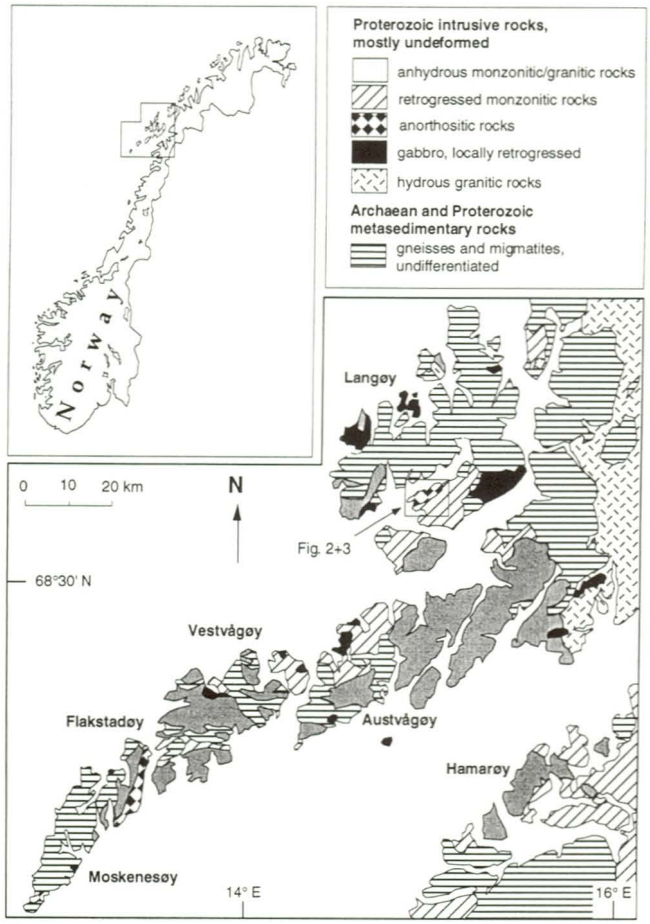

Fig. 1. Geological map of the Lofoten Islands in Nordland, modified after Griffin et al. 1978.

investigated the layered Hovden intrusion on Langøy which consists of rocks of gabbroic to mangeritic composition. His work focused on the Fe-Ti deposits in this intrusion and it is not clear whether the Hovden intrusion is temporally, spatially or genetically related to the Eidsfjord complex. The entire Eidsfjord anorthosite complex is thrust over the mainly monzonitic country rocks to the south, and hence does not show primary igneous contacts with them.

The phase assemblages of the Flakstadøy Basic Complex (FBC) and four samples of the Eidsfjord anorthosite have been described in detail by Markl et al. (1998). Markl & Frost (in press and submitted) showed, based on partition coefficient calculations and radiogenic isotope geochemistry, that the ferrodiorites from Lofoten may be regarded as the residual liquids of the anorthosites, which evolved by fractionation and assimilation of anatectic melts from the country rocks towards the compositions of the Lofoten mangerites and charnockites. At this time, the Eidsfjord anorthosite had been studied only on a reconnaissance level. During the 1997 field season, however, the Eidsfjord anorthosite was mapped and sampled in greater detail (Figs. 2 and 3) and the aim of the present paper is to present and interpret the new field and geochemical data. They support the model for the origin of the Lofoten-Vesterålen anorthosites proposed by Markl et al. (1998) and Markl & Frost (1998).

Field observations and sample description

Macroscopic petrography

The Eidsfjord region was mapped by Heier (1960) in a reconnaissance study of the rocks of the island of Langøy. He distinguished massive monzonitic rocks in the southern and southwestern part of the area from anorthosite in the northwestern, central and eastern part. In their investigation on mangerites and charnockites from the Lofoten-Vesterålen area, Malm & Ormaasen (1978) did not study the monzonitic rocks at the southern side of the Eidsfjord in any detail. They adopted the map produced by Heier (1960), which was also followed by Tveten (1978) on his map of the geology of the

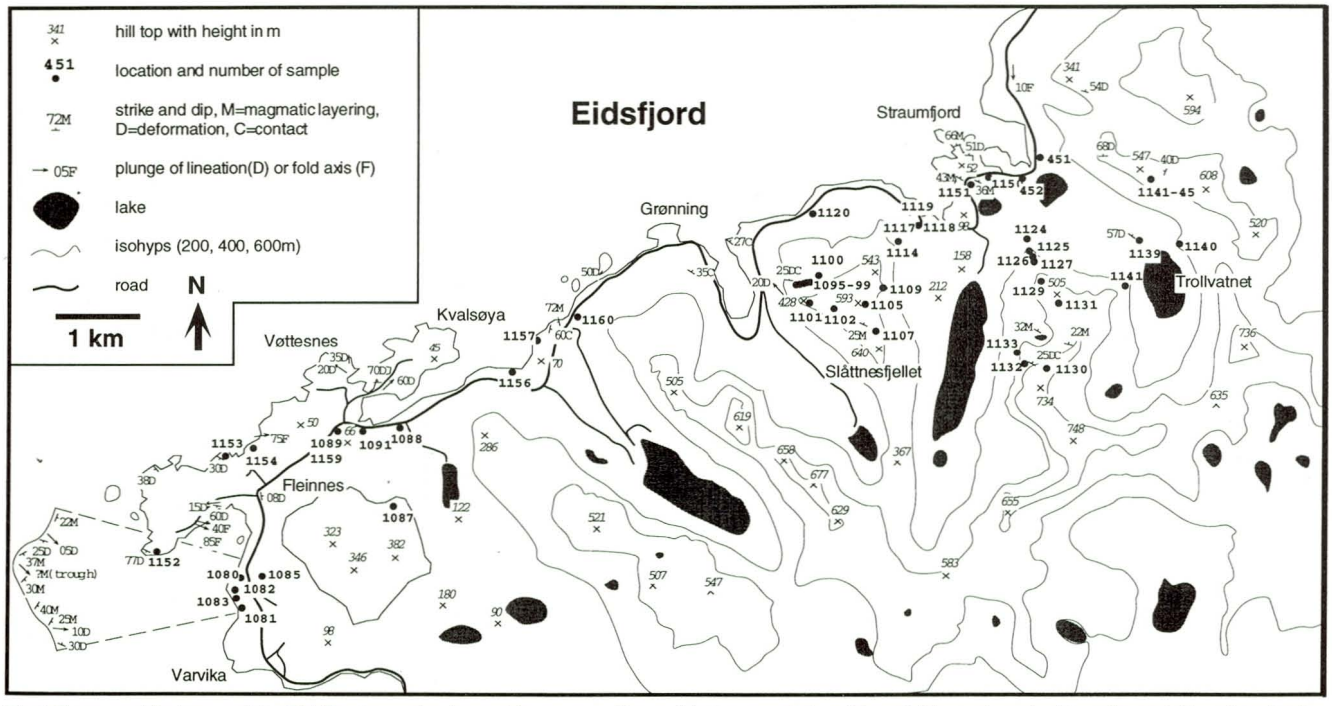

Fig. 2. Topographical map of the Eidsfjord anorthosite and its surroundings with the sample localities of this study and with strike and dip values for foliation planes, magmatic layering and contacts.

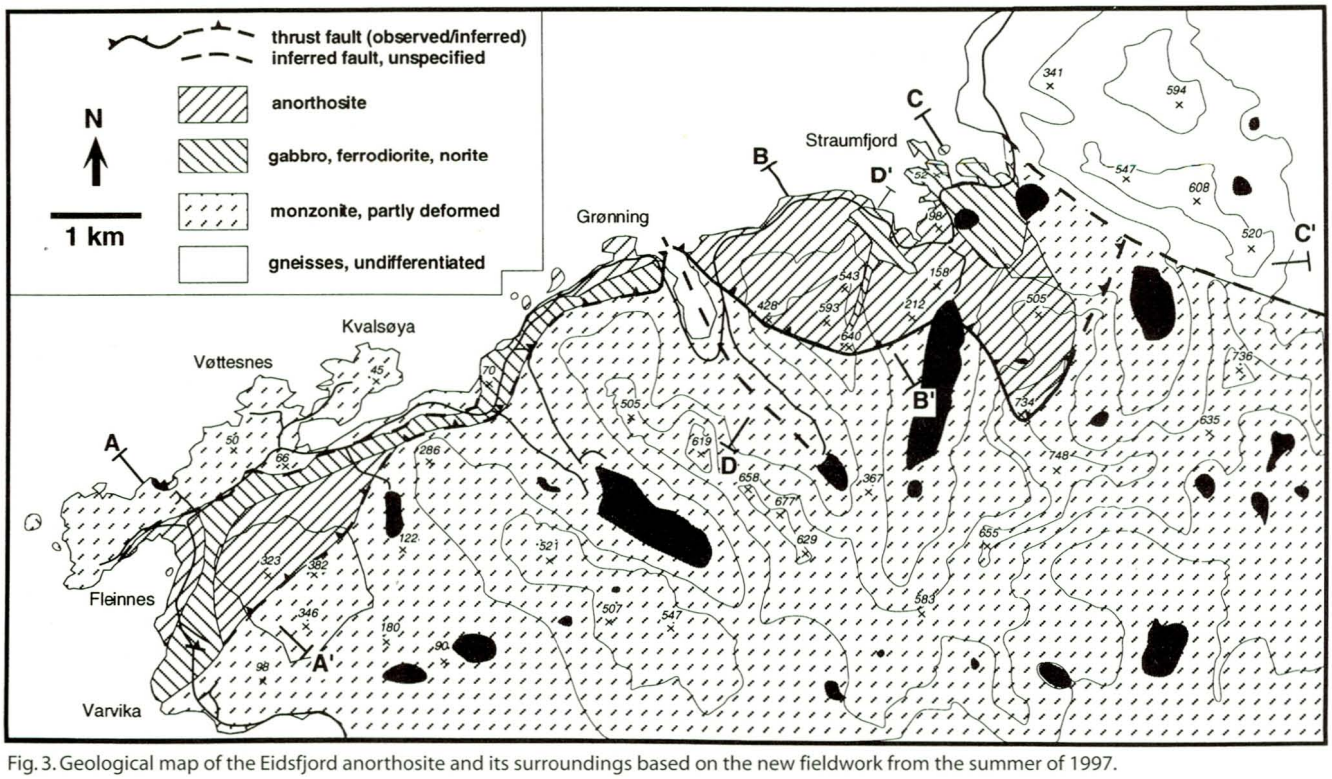

Fig. 3. Geological map of the Eidsfjord anorthosite and its surroundings based on the new fieldwork from the summer of 1997.

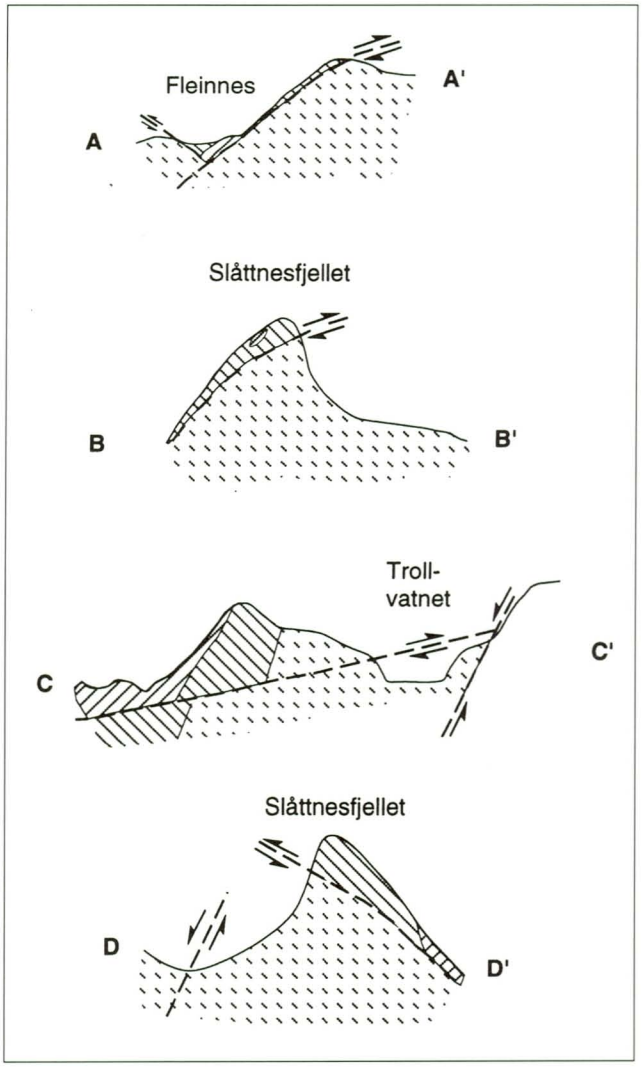

Fig. 4. Geological cross-sections through the Eidsfjord anorthosite complex. See Fig. 3. for location of the section lines.

sample	$X_{An}^{in\ Fsp}$	$X_{Or}^{in\ Fsp}$	$X_{en}^{in\ Cpx}$	$X_{En}^{in\ Opx}$	$X_{Fe}^{whole\ rock}$
GM 451	0.28	0.15	0.39-0.42	-	0.74
GM 452	0.44-0.46	0.02-0.03	0.57	0.67	-
GM 1080	0.25	0.20	-	-	0.73
GM 1081	0.25	0.12	-	-	0.65
GM 1082	0.25	0.11	0.44-0.5	0.6-0.61	0.63
GM 1083	0.29	0.06	?	-	0.69
GM 1085	0.4-0.41	>0.01	0.41-0.42	0.58-0.59	-
GM 1087	0.27	>0.02	0.38-0.39	0.47-0.51	-
GM 1088	0.39	>0.01	-	0.58-0.59	-
GM 1089	0.33-0.41	>0.01	-	-	-
GM 1091	0.37	>0.02	0.41	0.56-0.58	-
GM 1096	0.53-0.56	>0.01	0.44-0.45	0.64-0.66	-
GM 1099	0.52-0.58	>0.01	0.44	0.64-0.67	-
GM 1100	0.54-0.58	>0.01	?	0.64-0.65	-
GM 1105	0.52-0.57	>0.02	0.41-0.45	0.64-0.67	-
GM 1107	0.44-0.46	>0.02	-	0.64-0.66	-
GM 1109	0.49-0.8	>0.01	-	0.66-0.67	-
GM 1114	0.45-0.47	>0.02	-	0.63-0.65	-
GM 1117	0.38-0.4	>0.02	0.44	0.61-0.63	-
GM 1118	0.49-0.54	>0.02	0.46	0.64-0.65	-
GM 1119	0.44-0.86	>0.02	0.43-0.44	0.65-0.66	-
GM 1120	0.17	0.21	0.45-0.47	-	0.69
GM 1124	0.39-0.44	>0.01	0.42-0.43	0.58	-
GM 1125	-	-	-	0.68-0.69	-
GM 1126	0.68-0.8	0.03	0.40-0.43	-	0.54
GM 1127	0.69	0.05	0.48	-	0.52
GM 1129	0.48-0.56	>0.2	0.44-0.47	-	-
GM 1130	0.52-0.55	>0.02	0.44-0.47	0.64-0.65	-
GM 1131	0.56-0.57	>0.01	0.42-0.44	0.63-0.65	-
GM 1132	0.52-0.58	>0.02	-	0.62-0.64	-
	-	-	0.38	0.51	-
GM 1133	0.55-0.58	>0.01	0.43-0.48	0.6-0.61	-
GM 1139	?	?	0.35-0.36	0.46-0.48	-
GM 1140	0.08	0.36	0.34-0.35	0.44-0.45	0.79
GM 1141	0.18	0.16	0.38-0.4	0.51-0.52	0.73
GM 1145	0.48	0.09	-	-	0.56
GM 1150	0.41-0.49	>0.02	0.41-0.43	0.62-0.65	-
GM 1151	0.49-0.51	>0.02	0.43	0.62-0.65	-
GM 1152	0.12-0.17	0.24-0.4	0.42-0.44	-	-
GM 1153	0.34-0.36	>0.01	0.42-0.44	0.56-0.57	-
GM 1154	0.28	0.10	-	-	0.67
GM 1156	0.07	0.38	-	-	0.81
GM 1157	0.54-0.56	>0.01	0.47	-	-
GM 1159	0.16	0.21	0.37-0.40	0.49	0.73
GM 1160	0.26	0.09	0.41-0.44	0.58-0.59	0.67
GM 1161	-	-	0.38-0.39	0.52-0.53	-

Table. 1. Mineral chemistry of the samples used in this study.

Lofoten-Vesterålen district. In the present study, a total of 81 samples were collected and studied in thin-section, of which 40 were polished and used in electron microprobe investigations. XRF analyses were performed on 15 of the samples. Hence, this study is the first to investigate the Eidsfjord anorthosite in detail.

The results of the new mapping from the summer of 1997 are presented in Figs. 2, 3 and 4. The structural interpretation of the anorthosite complex is now considerably different from the one suggested in the previous studies. The map of Fig. 2 shows the sample localities of the present study, Tables 1 and 2 present data on the mineral assemblages, the mineral chemistry and the rock types of each sample and Figs. 3 and 4 show the actual mapping results. There are two different anorthositic rock types in the complex, the contacts between which are usually gradational but can be well distinguished in outcrop: pure, blackish (fresh) or whitish (weathered), coarse-grained anorthosite s. s., and a leuconoritic to noritic rock with a significantly higher content of mafic minerals (called leuconorite in this paper). Both rock types are of variable grain-size ranging from very coarse-grained to extremely fine-grained. In places, both rock types show lenses and stringers of pyroxenites, but only the more mafic type may contain rounded lenses which almost exclusively consist of Fe-Ti oxides and Fe- and Fe-Cu sulphides. In some outcrops, the noritic rocks appear to grade into ferrodiorites that are even more mafic, very oxide-rich and typically very fine-grained apart from some large feldspar phenocrysts. Commonly, however, the ferrodiorites are younger than the leuconorites and occur as veins and dykes up to a few metres wide at the most. The anorthosite in some outcrops on the northeastern slope of hill 543 m west of Straumfjord (Fig. 2) contains fractures filled with pyroxenite

sample	XRF	rock type	primary magmatic mineral assemblage												notes
			Plag	Kfsp	Msp	Opx	Cpx	Pig	Ol	Mt	Ilm	Py	Po	Ap	
GM 451	x	ferrodiorite	x		(x)	x	x			x	x			x	
GM 452		anorthosite	x			x	x			x	x			x	
GM 1080	x	ferrodiorite	x			x	x			x	x			x	
GM 1081	x	ferrodiorite	x			x	x			x	x			x	
GM 1082	x	norite	x			x	x			x	x	x		x	
GM 1083	x	ferrodiorite	x		(x)	x	x			x	x			x	
GM 1085		ferrodiorite	x			x	x			x	x			x	
GM 1087		norite	x			x	x			x	x			x	
GM 1088		norite	x			x				x	x	x		x	
GM 1089		oxide-sulphide lens	x							x	x	x			
GM 1091		anorthosite	x		(x)	x	x			x	x			x	
GM 1096		anorthosite	x			x	x				x			x	
GM 1099		anorthosite	x			x	x			x	x			x	
GM 1100		anorthosite	x			x				x	x			x	
GM 1105		anorthosite	x			x	x			x	x			x	
GM 1107		oxide- sulphide lens	x			x				x	x	x		x	Cpy
GM 1109		oxide- sulphide lens	x			x	x			x			x	x	Qtz
GM 1114		pyroxenite	x			x				x	x				
GM 1117		norite	x			x	x			x	x				
GM 1118		anorthosite	x			x	x			x	x			x	
GM 1119		oxide- sulphide lens	x			x	x			x		x	x		
GM 1120	x	monzonite			x		x		x	x	x			x	
GM 1124		ferrodiorite	x			x?	x			x	x			x	
GM 1125		pyroxenite				x					x	x	x		
GM 1126	x	gabbro	x				x		x		x				
GM 1127	x	gabbro	x				x		x		x				
GM 1129		anorthosite	x			x	x			x	x			x	
GM 1130		anorthosite	x			x	x			x	x			x	
GM 1131		anorthosite	x			x	x		(x)	x	x			x	Opx ps. a. Ol?
GM 1132		anorthosite	x			x	x		(x)	x	x			x	Opx ps. a. Ol
		monzonite			x	x	x			x	x			x	
GM 1133		anorthosite	x			x	x			x	x				
GM 1139		monzonite			x	x	x			x	x			x	
GM 1140	x	monzonite			x	x	x			x	x			x	
GM 1141	x	monzonite			x	x	x			x	x			x	
GM 1145	x	gabbronorite	x			x	x			x	x			x	
GM 1150		ferrodiorite	x		x	x	x			x	x			x	
GM 1151		pyroxenite	x			x	x			x	x			x	
GM 1152		monzonite			x		x			x	x			x	
GM 1153		norite	x			x	x			x	x			x	
GM 1154	x	norite	x			x	x			x	x			x	
GM 1156	x	monzonite			x	x	x			x	x			x	
GM 1157		gabbro	x				x		x	x	x	x			
GM 1159	x	monzonite			x	x		x		x	x			x	Qtz
GM 1160	x	norite	x			x	x			x	x				
GM 1161		norite	x			x	x			x	x			x	

Table 2. Mineral assemblages of the samples used in this study. For sample locations, see Fig. 2.

(Fig. 5 A and B). This indicates that a very pyroxene-rich crystal mush intruded the brittly deforming anorthosite.

While some of the mafic rocks are contemporaneous with the anorthosite, others are evidently younger. This is proven by the occurrence of xenoliths of anorthosite in ferrodiorites in a road-cut at Storeset near Straumfjord (Fig. 5 C). A few veins of monzonitic to granitic (with quartz, Fe-Ti oxides and pyroxenes) and of ferrodioritic composition were found cross-cutting the anorthosite and the norites.

The mafic rocks are easily spotted in the field due to their rusty brown colour (in contrast to the whitish weathering colours of the anorthosites). The largest accumulation of mafic rocks occurs between Straumfjord and hill 505 m to the southeast. Large and abundant masses of Fe-Ti oxides and sulphides occur along the road immediately to the west of the bay of Straumfjord, and another occurrence was found in the road-cut where the road Fleinnes-Grønning meets the small road from Kvalsøya (Fig. 2). Very large pyroxenes (up to 0.5 m) and up to 30 m large lenses of pyroxenites occur in the slope above the oxide-sulphide lenses on the northeastern slope of hill 543 m (see Fig. 2). In the western part of the complex near Fleinnes, the noritic rocks occur in a zone bet-

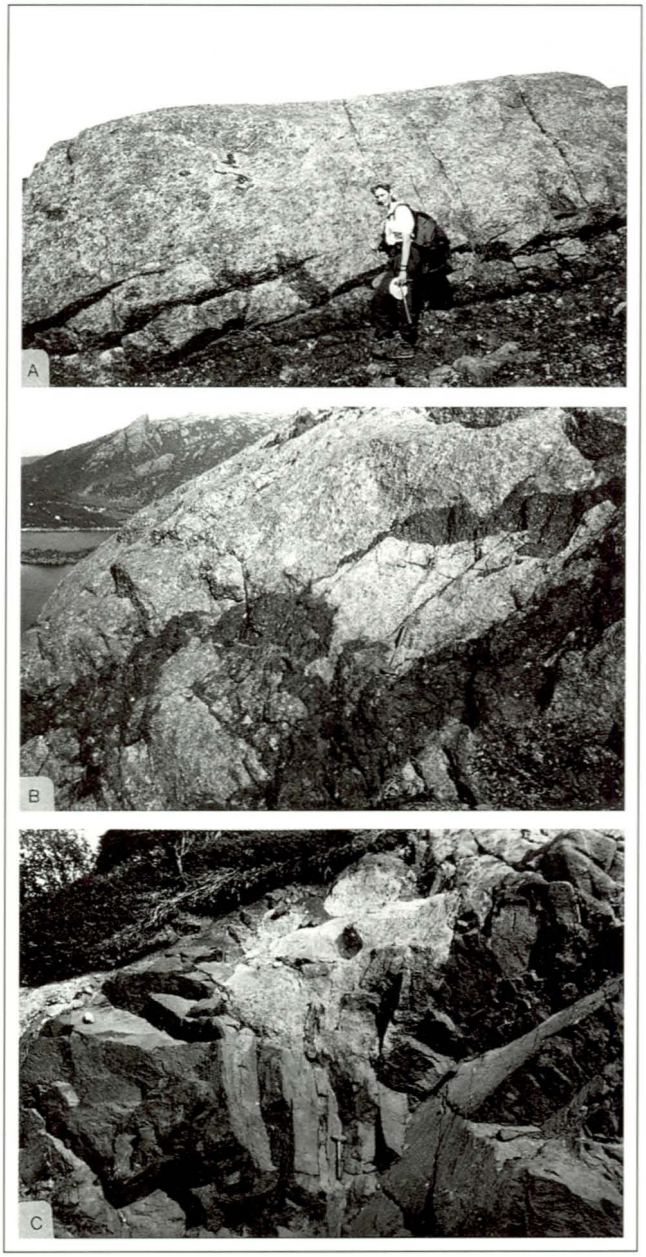

Fig. 5. (A) A virtually pure lens of orthopyroxenite (dark, bottom) in anorthosite s. s. (light grey, top). Note the 'apophyses' of the pyroxenite in the anorthosite (the largest one is about 50 cm left of the person). Northeast slope of hill 543 m west of Straumfjord. (B) Dark orthopyroxenite fills fractures in light grey anorthosite at the same locality. The hammer is about 60 cm long. (C) Xenolith of anorthosite (lighter grey, centre) in noritic to ferrodioritic rocks. Road-cut near Ytterneset/ Straumfjord.

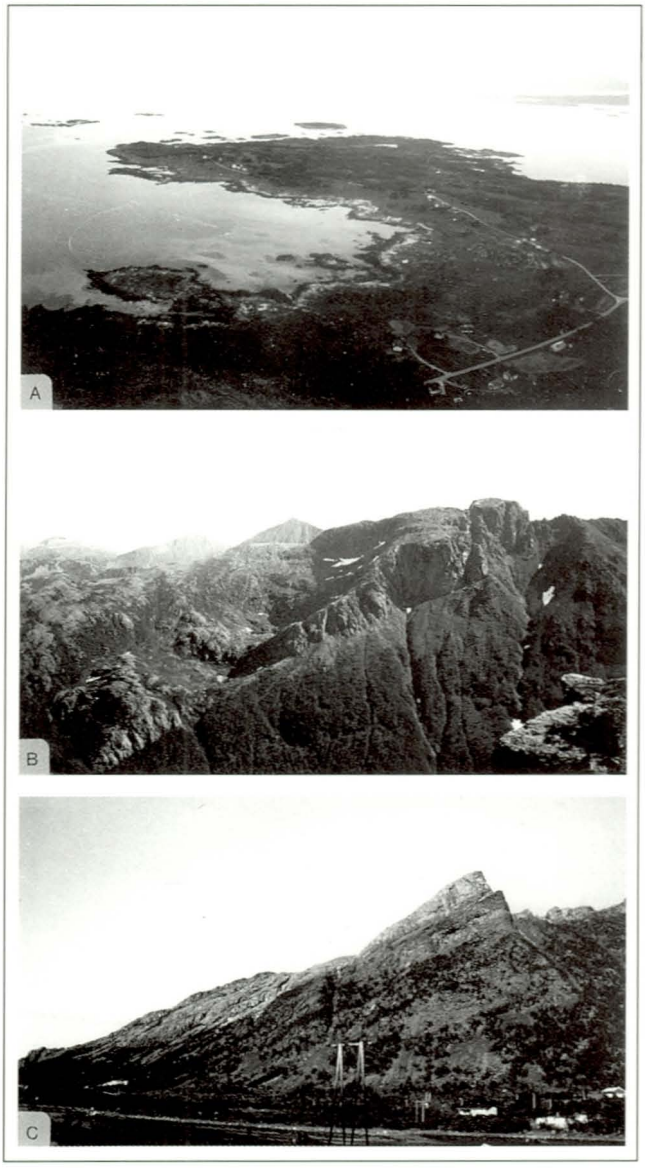

Fig. 6. (A) The bay of Fleinnes in the Eidsfjord anorthosite; the peninsula in the background (reaching into the Eidsfjord) consists of monzonitic rocks whereas the inner part of the bay and the small peninsula in the foreground are composed of anorthosite and gabbronorite. Note the houses in the foreground for scale. (B) The massive, grey anorthosite is overthrust over monzonitic rocks south of Straumfjord. The view is from the west towards the hill 734 m (see Fig. 2). Note the clear-cut fault zone at the base of the anorthosite. (C) View from the west towards the hill 428 m on the eastern side of the small bay south of Grønning (Fig. 2). A thin, light-grey slice of anorthosite is thrust over the monzonitic rocks below; at this locality, the fault zone consists of about 40 m of monzonitic mylonites and ultramylonites. Note houses for scale.

ween two patches of anorthosites. The lower of these two patches of anorthosite, which crops out in the bay of Fleinnes (Fig. 6 A), is strongly overprinted by an amphibolite-facies metamorphic event, but still shows magmatic textures. These textures are unlike the ones found in the rest of the complex. Specifically, large quadrangles of plagioclase up to 10 cm in size 'float' in a groundmass of plagioclase of 1-2 cm size with some mafic interstitials. It is also this part of the anorthosite that exhibits the only magmatic layering in the complex (except for one single example near Straumfjord). The upper part of this anorthosite appears to be very similar to the main anorthosite in the centre of the complex.

The field appearance of the monzonitic rocks on the peninsula between Fleinnes and Kvalsøya is identical to the monzonites found on the shore south of Kvalsøya and in the south of the anorthosite complex. These rocks differ, however, from the monzonitic rocks in the valley southeast of

Straumfjord in that they are coarser grained (feldspars up to 4 cm in contrast to about 1 cm) and also contain abundant biotite rather than pyroxenes. The monzonitic rocks from the valley southeast of Straumfjord are younger than or at least coeval with the anorthosite. This is proven by a ca. 5 cm large xenocryst of typical anorthositic plagioclase that was found within the mangerite at one locality (in the cliff northeast of Trollvatnet) .

The borders of the complex against the underlying monzonite are well exposed in the form of a huge thrust fault (see below) in the southeastern and central part of the complex (Fig. 6 B and C). Strongly deformed monzonite-anorthosite contacts are also exposed on the northern shore of Fleinnes bay. The eastern border of the complex against the gneisses, however, is covered with scree and vegetation and only a few lenses of gneiss are found on the small peninsula near Straumfjord. In the east, the outermost outcrops consist of garnet-diopside-scapolite-bearing calc-silicate rocks. The rest of the gneisses, as described by Heier (1960), are of variable, but commonly mafic composition and generally show two-pyroxene assemblages.

Magmatic layering

Magmatic modal layering was observed in one road-cut at Straumfjord where it dips at 35 ° to the northeast, and it is especially well developed along the coast to the south of Fleinnes (Fig. 7). Here, it generally dips at 20-40 ° to the southeast. At one locality along this coast, a structure was found that appears to be a magmatic trough which plunges to the southeast.

Deformation

The most prominent feature of the Eidsfjord anorthosite is that the entire complex is thrust over monzonites and monzonitic gneisses that crop out to the south and to the northwest (Figs. 2 and 3). In the central part east and southeast of Grønning and south of Straumfjord, this movement is recorded by a ca. 40 m-thick mylonite zone (Fig. 6 B and C), which partly contains ultramylonites. This mylonite zone dips gently (~ 25 °) to the northeast with a lineation plunging at 20° to the northwest. The ductile deformation was completely confined to the underlying monzonite, whereas the anorthosite above shows abundant pseudotachylites. The abundance of the latter decreases from more than 50% of the whole rock within the first 5 m above the mylonite zone to virtually zero about 50 m above the zone. However, small 'vein-like' pseudotachylites are found throughout the entire anorthosite complex.

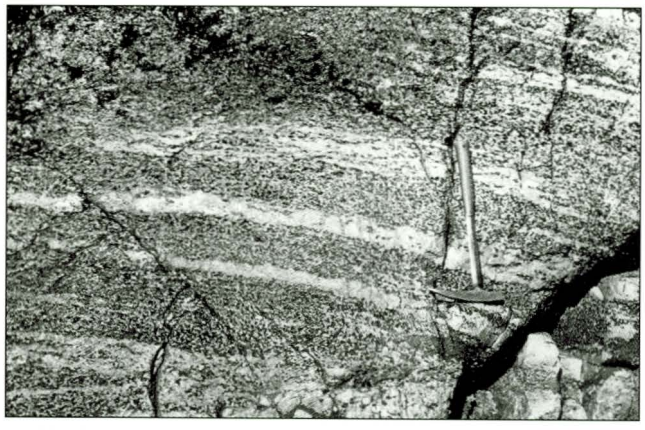

Fig. 7. Magmatic layering with alternating layers of anorthositic and gabbronoritic composition. Bay of Fleinnes. The hammer is about 60 cm long.

Around Fleinnes, the anorthosite is strongly deformed in a ductile manner. As shown in Fig. 2, lineations plunge gently to the southeast south of the bay to gently to the west north of the bay. The foliation generally dips gently to steeply to the southwest or northeast. West of Grønning, the foliation in the deformed anorthosite dips at 50° to the northwest, and along the eastern margin of the anorthosite east and southeast of Straumfjord, foliation dips 50-60° to the north and northeast. Generally, therefore, the foliation in the country rocks to the north of the complex appears to surround the anorthosite. As the deformation was accompanied by metamorphic reactions that produced amphibole and biotite at the expense of the pyroxenes, the foliation is believed to be related either to the 1.1 Ga or the Caledonian amphibolite-facies regional metamorphic event (Griffin et al. 1978, Hames et al. 1996). The contact of the anorthositic rocks both with the monzonitic rocks between Fleinnes and Kvalsøya and with the gneisses east of the complex is tectonic.

Kinematic indicators (e. g. deformed and rotated feldspars south of Straumfjord) suggest that the direction of movement along the mylonite zone was top to the south or southwest. Based on the field relations, however, it is not clear how far the anorthosite was transported. The observation in the valley southeast of Straumfjord that the mangerite there extends above and below the fault, which is developed as a very small (few metres thick) zone of weak deformation, may indicate that the anorthosite was not moved very far, perhaps in the order of a few to a few hundred metres (see e. g. cross-section C-C' of Fig. 4). However, the outcrops in this valley with dense, abundant vegetation do not allow an unequivocal assessment of transport distance.

Sample descriptions

The samples of this study are listed in Table 2 with regard to their rock type and their mineral assemblage. Only the general characteristics of the observed rock types are described here.

Anorthosites s. s. and leuconorites show large laths of plagioclase up to 30 cm across, with variable amounts of interstitial pyroxenes and Fe-Ti oxides. In thin-section, the plagioclase crystals are commonly recrystallized at their rims. Zoning or iridescence have not been observed. The pyroxenes are typically exsolved showing either abundant exsolution lamellae of a few microns to more than 30 microns thickness or blebby exsolutions preferentially congealed along

the rims of the former host. Reintegration of the original composition of two coexisting pyroxenes was in all but one case unsuccessful (i. e. it gave results indicating low-temperature reequilibration). The oxides in most cases show strong flame-like exsolution and oxidation features, and reintegration was not attempted.

Mafic rocks include the entire spectrum ranging from gabbronorites and norites to ferrodiorites. They show a framework of plagioclase or mesoperthitic feldspar with interstitial pyroxenes, Fe-Ti oxides and rarely olivine. Especially in the ferrodiorites, euhedral apatite is common and it is generally associated with the oxide phases. Blebby exsolutions of K-feldspar in plagioclase (antiperthite) are observed in almost every sample though in highly variable amounts. Pyroxenes are exsolved as described above. When present, olivine is always surrounded by a rim of tabular orthopyroxene which, based on the texture, may be of magmatic origin.

Monzonitic rocks show large grains of ternary, mesoperthitic, alkali feldspar that is strongly exsolved. In some cases, these fishbone-like exsolutions are so fine that reintegration of the original magmatic feldspar composition with a broad beam on the microprobe was possible. Pyroxenes (including inverted pigeonite) and Fe-Ti oxides occur as anhedral grains and show the exsolution features as described above. Some of the samples show large amounts of brown secondary biotite and green amphibole rimming and replacing the primary pyroxenes.

Whole-rock geochemistry

Analytical techniques

XRF analyses were carried out at the Institut für Mineralogie, Petrologie und Geochemie at the Universität Freiburg, Germany, on a Philips PW 1450/20 instrument with natural standards; for Cl measurements, the international standards BR (with 350 ppm Cl) and NIM-L (with 1200 ppm Cl) were used. The raw data were processed with the standard XR-55 software of Philips; accuracy and detection limits are on the order of 0.1% for major elements and 1-10 ppm (depending on the specific element) for minor elements, respectively. Table 3 presents whole-rock chemical data of the Eidsfjord rocks. The XRF analyses were obtained from powders dried at 105°C. After measurement, Fe^{2+} was determined by titration.

sample no.	GM 451	GM 1080	GM 1081	GM 1082	GM 1083	GM 1120	GM 1126	GM 1127
SiO_2	45.89	42.27	46.76	48.18	43.74	45.40	48.70	44.80
TiO_2	2.92	2.61	1.96	1.98	2.45	2.57	1.16	1.25
Al_2O_3	14.00	15.31	15.32	15.44	16.26	15.02	14.96	17.06
Fe_2O_3	9.18	6.35	8.17	8.43	9.35	6.23	5.03	1.06
FeO	7.98	11.16	9.23	8.45	7.66	9.35	8.60	10.81
MnO	0.18	0.19	0.18	0.17	0.16	0.21	0.21	0.15
MgO	3.54	5.35	6.31	6.25	4.38	5.37	9.49	12.68
CaO	7.44	8.86	6.59	7.03	9.95	7.68	12.26	10.64
Na_2O	3.37	2.96	3.32	3.45	3.48	3.8	1.27	1.87
K_2O	1.98	1.63	0.98	0.88	0.45	1.97	0.15	0.30
P_2O_5	0.78	1.82	0.54	0.49	1.91	1.67	0.04	0.06
Total	97.26	98.51	99.36	100.80	99.79	99.27	101.90	100.70
Rb	28	23	10	9	7	22	6	6
Sr	595	632	729	710	897	841	123	90
Ba	2119	280	805	811	386	1527	51	115
Pb	9	14	16	12	11	33	29	17
Y	32	19	16	15	26	38	21	21
Nb	7	4	4	5	4	7	4	5
Zr	109	6	34	12	b. d. l.	90	23	32
V	424	455	411	450	219	244	321	350
Ni	17	56	53	12	3	30	71	114
Cr	16	95	233	96	94	37	274	395
Co	46	44	47	34	24	40	48	43
Cu	20	50	46	33	17	30	37	10
Zn	144	169	205	163	198	167	110	110
Ga	23	19	16	16	17	14	12	12
Th	n. d.	4	4	6	6	8	7	5
Sc	26	20	17	13	16	17	22	20
La	41	25	14	18	16	24	b. d. l.	b. d. l.
Cl	n. d.	391	222	b. d. l.	407	b. d. l.	b. d. l.	b. d. l.
S	n. d.	709	797	624	294	812	1431	240
FeO/(FeO+MgO)	0.69	0.68	0.59	0.57	0.64	0.64	0.48	0.46

n. d. - not determined; b. d. l. - below detection limit

Table 3. XRF analyses of fine-grained rocks from the Eidsfjord anorthosite complex.

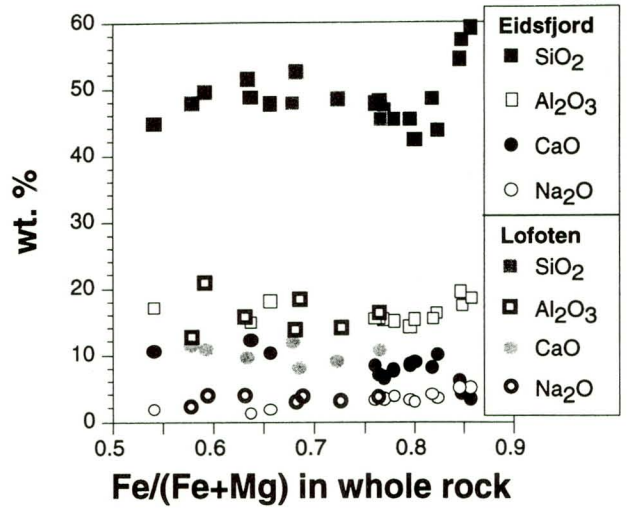

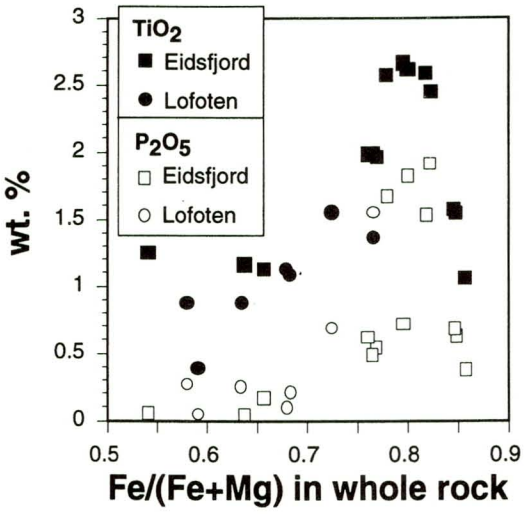

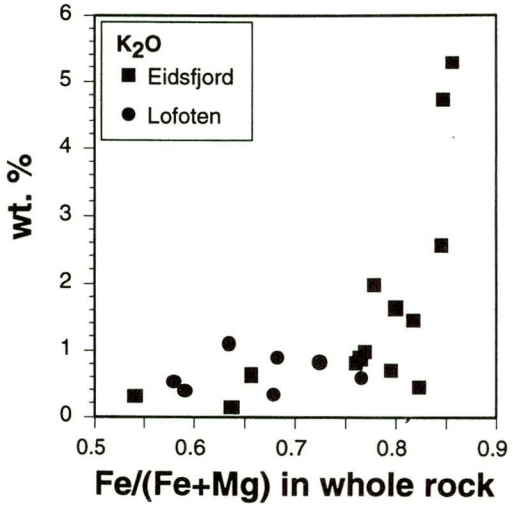

Fig. 8. Some major and minor elements of the Eidsfjord rocks plotted against XFewhole rock. See text for discussion.

Major and minor elements

Figure 8 shows major and minor elements of whole-rock samples from the Eidsfjord anorthosite plotted against their X_{Fe} (molar $Fe^{2+}/(Fe^{2+}+Mg)$) value, which is, as Fig. 8 shows, a better indicator of fractionation than e. g. the SiO_2 content. Whole-rock analyses of gabbroic and ferrodioritic rocks from other parts of the Lofoten Islands (reported in Markl & Frost, in press) are also shown for comparison.

The data show the following important features:

- the Eidsfjord rocks show trends comparable to the trends spanned by the rest of the Lofoten rocks.
- SiO_2 stays relatively constant during fractionation from the most primitive gabbro with an X_{Fe} of 0.54 to ferrodiorite with X_{Fe} values below 0.75, and it shows a low point in the evolved ferrodiorites before it increases drastically in the monzonitic rocks.
- Al_2O_3 shows considerable scatter in the gabbroic varieties, but it decreases until the lowest value is reached in the evolved ferrodiorites from which Al_2O_3 increases towards the monzonites with high X_{Fe}.
- CaO and Na_2O show steady decreases (CaO) or increases (Na_2O), respectively, during the whole fractionation interval. MgO and FeO^{tot}, which are not plotted, show decreases (MgO) and increases (FeO^{tot}) if plotted against X_{Fe}, but FeO^{tot} shows a very pronounced high in the evolved ferrodiorites with X_{Fe} around 0.8.
- P_2O_5 and TiO_2 form two identically shaped trends from low values in low X_{Fe} rocks to maxima in the evolved ferrodiorites, and with a strong decrease towards the monzonites.
- K_2O shows a more or less steady increase towards the ferrodiorites before it is finally strongly enriched in the monzonites.

Trace elements

If plotted against X_{Fe}, many of the trace elements show clear trends, but some of the trace element patterns are considerably more scattered (Fig. 9). This may either point to the involvement of cumulate processes or it may reflect, as perhaps in the case of Sr, a disturbance during later metamorphism, eventhough the samples were chosen based on their

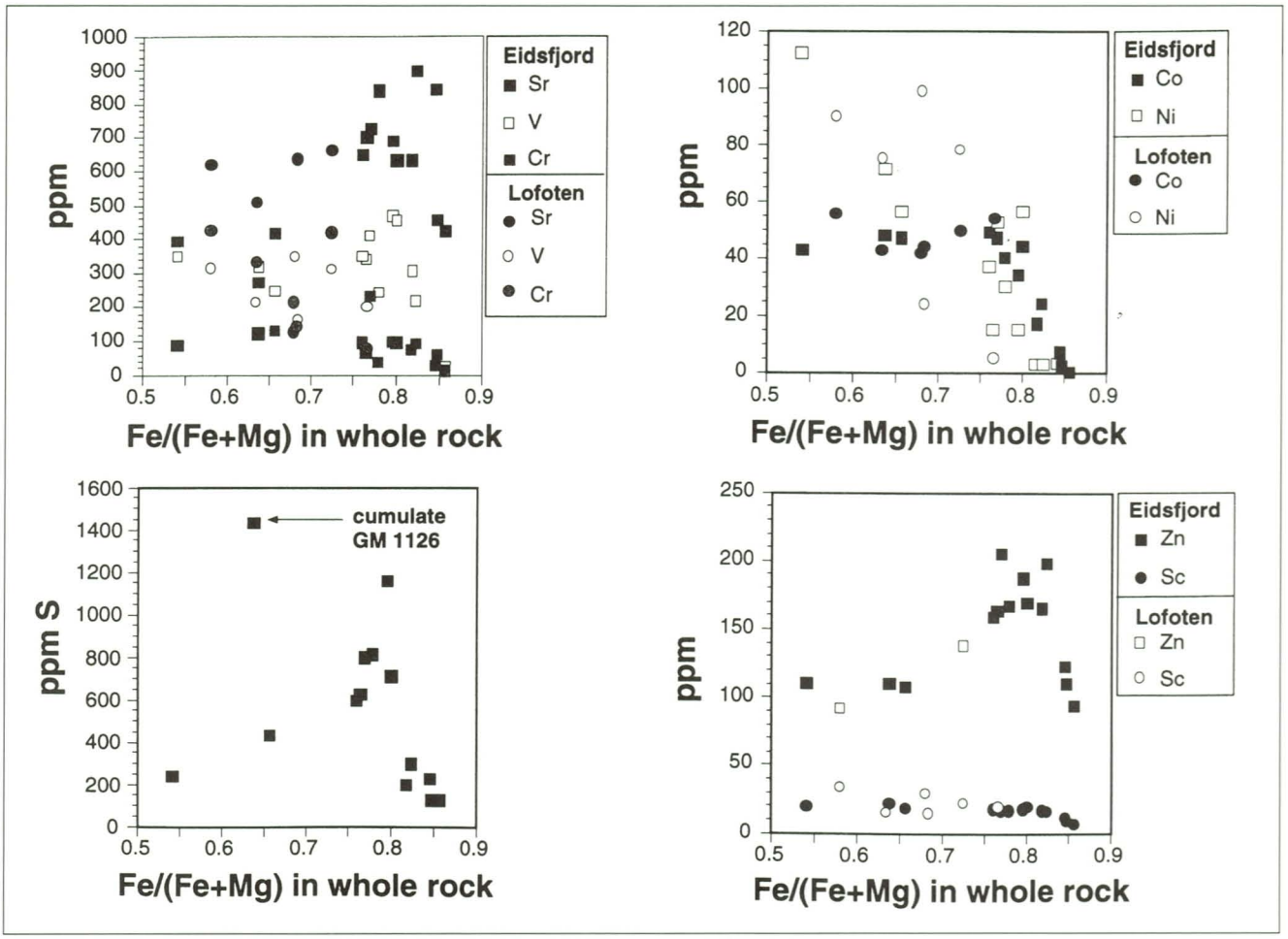

Fig. 9. Some trace elements of the Eidsfjord rocks plotted against XFewhole rock. See text for detailed discussion.

fine-grained nature and their fresh, unaltered and unmetamorphosed appearance. The various investigated trace elements behave as follows:

- Sr shows a wide scatter in the most primitive gabbros but generally increases towards the ferrodiorites and shows lower values in the monzonites.
- V scatters between 150 and 450 ppm in the entire fractionation interval, and apart from the monzonites, which contain virtually no V, there is no distinctive trend visible. Even in the very oxide-rich ferrodiorites with X_{Fe}=0.8, in which V would be expected to be enriched during cumulate processes, it ranges from 200 to 450 ppm and hence argues against a cumulate origin for the evolved ferrodiorites.
- Cr shows a more or less monotonous decrease from about 400 ppm in the gabbros to virtually zero values in the monzonites.
- Co and Ni show very interesting trends: whereas Co remains approximately constant at about 50±10 ppm in the gabbros and low-X_{Fe} ferrodiorites, it starts to decrease significantly at X_{Fe} values of 0.75 and higher. Ni, in contrast, decreases like Cr monotonously from 120 to 0 ppm in the entire X_{Fe} interval.
- Interestingly, Zn shows a pattern very similar to the Ti and P patterns (Fig. 8), showing an increase towards the very Zn-rich evolved ferrodiorites with a low in the monzonites. Sc, in contrast, shows a monotonous decrease from gabbros towards monzonites.
- S follows the patterns for Ti, P and Zn and shows clear highs in the evolved ferrodiorites. One pyroxenitic cumulate of relatively low X_{Fe} (which is not plotted in the other whole-rock chemistry diagrams) with about 1400 ppm S is exceptional.
- REE data for one ferrodioritic sample (GM 451) have been reported in Markl & Frost (in press). It shows a smoothly decreasing pattern without any significant Eu anomaly.

Figure 10 plots some trace elements against some minor elements. There is a scattered, but obvious correlation between Rb and K_2O and a much stronger one between Ba and K_2O. Ba reaches maximum values of almost 3000 ppm and Rb of 40 ppm in the monzonites. La shows a good correlation with P_2O_5 at low values of P_2O_5 and one sample of the very P_2O_5-rich rocks is also in agreement with the same trend. However, there is a distinct group of high-P_2O_5 rocks (evolved ferrodiorites, see Fig. 8) with low La values.

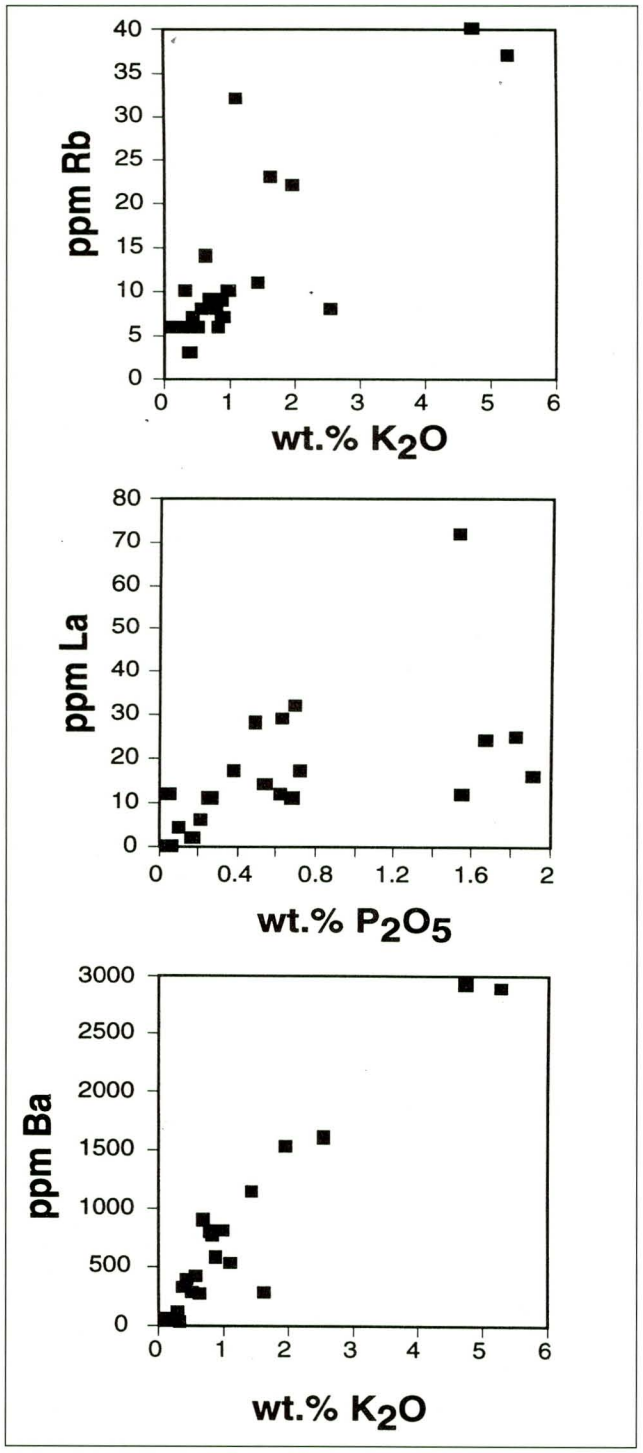

Fig. 10. Correlation diagrams between some minor and trace elements from the Eidsfjord rocks. See text for discussion.

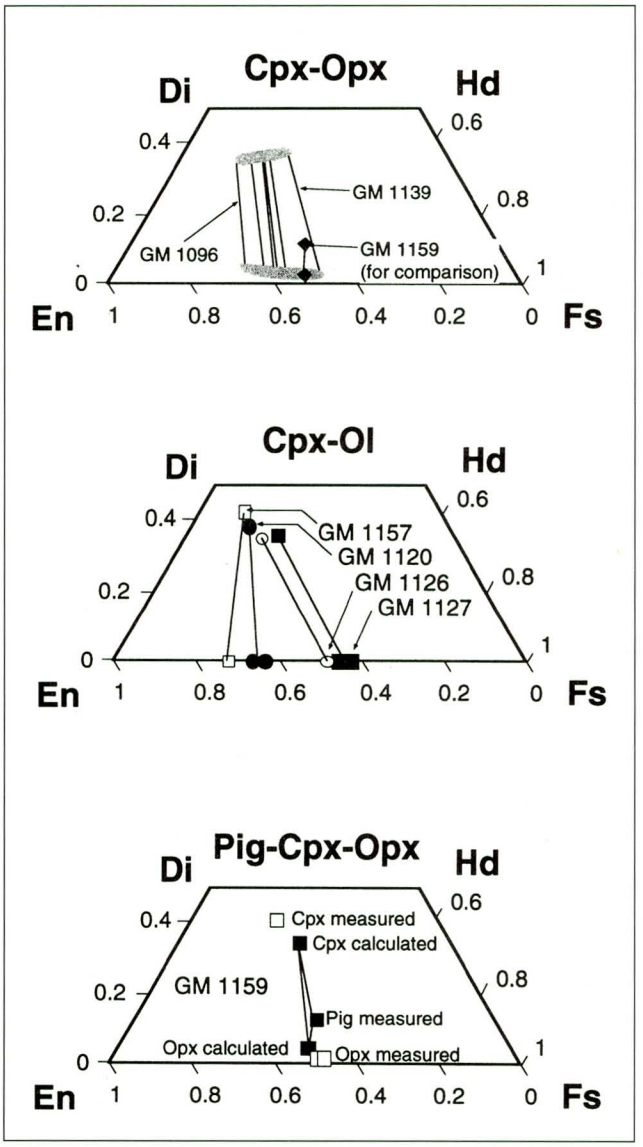

Fig. 11. Microprobe measurements of pyroxenes and olivine plotted into the pyroxene quadrilateral after the projection scheme of Lindsley (1983). The pyroxene/olivine assemblages observed in the Eidsfjord rocks are shown in separate diagrams; in the pig-involving sample, the measured and the calculated mineral compositions are separately plotted for comparison. For a detailed discussion see the text.

Mineral chemistry

Analytical methods

Wavelength dispersive electron microprobe analyses were performed on a CAMECA SX100 at the Institut für Mineralogie, Petrologie und Geochemie at the Universität Freiburg, Germany with internal PAP-correction (Pouchou & Pichior 1984, 1985). CAMECA-supplied natural and synthetic standards were used for most of the major and minor elements. Measuring times per element were 20 seconds (but for F, 60 seconds) with an emission current of 10 nA and an acceleration voltage of 15 kV. For F and Cl measurements in apatite, a Durango apatite with 3.53 % F and 0.41 % Cl was used as the standard in order to avoid problems with interfering P-lines.

Olivine

Olivine in 4 samples ranges in composition from Fo_{72} to Fo_{42}. The Mn content is variable (between 0.4 and 1.1 wt.%), but is not simply correlated to the Fo-content of the olivine, i. e. the most Fe-rich olivine does not exhibit the highest Mn content. Table 4 presents selected elec-

wt. %	1126-6 ol	1127-4 ol	1157-5 ol	1120-8 ol
SiO_2	34.13	35.96	38.32	34.50
FeO	46.48	30.61	24.81	43.79
MnO	0.67	0.29	0.38	1.09
MgO	18.90	33.44	36.30	20.30
CaO	0.01	0.00	0.00	0.00
Total	100.23	100.32	99.82	99.75
Formula based on 4 oxygens				
Si	1.00	0.97	1.01	1.01
Mg	0.83	1.35	1.43	0.88
Fe	1.14	0.69	0.55	1.07
Mn	0.02	0.01	0.01	0.03
Ca	0.00	0.00	0.00	0.00
Sum	3.00	3.03	2.99	2.99
Fa	58	34	28	55
Fo	42	66	72	45

Table 4. Selected microprobe measurements of olivine in four samples from the Eidsfjord anorthosite complex.

tron microprobe analyses of olivine, while Fig. 11 plots olivine together with the coexisting clinopyroxene in the pyroxene quadrilateral.

Orthopyroxene

In terms of the Lindsley (1983) projection, orthopyroxene in the investigated gabbroic, ferrodioritic and monzonitic rocks ranges in composition from $En_{72}Wo_1$ to $En_{45}Wo_2$. The highest measured Wo content is $En_{64}W_{04}$ in samples GM 1105 and GM 1096. As the rest of the orthopyroxenes are typically coarsely exsolved, the magmatic Wo content, which was significantly higher than the measured one, could not be determined. MnO contents range between 0.3 and 1.3 wt. % with the highest MnO contents in the most Fe-rich orthopyroxenes (Fig. 12). Al_2O_3 contents vary significantly between 0.3 and 3.3 wt. % and are well correlated to X_{En} (Fig. 12). TiO_2 contents are weakly correlated to the X_{Fe} of the orthopyroxene (Fig. 12) and range from 0 to 0.45 wt.%. Table 5 presents representative electron microprobe analyses of pyroxenes in samples GM 1159 and GM 1096 from the Eidsfjord rocks and Fig. 11 shows the quadrilateral plots with the observed mafic assemblages and with all analyses.

Inverted pigeonite

Inverted pigeonite was found to occur in one sample only (GM 1159, Fig. 11). It is exsolved in a way (very fine exsolution lamellae) that reintegration was possible by using a broad electron beam. The measured composition is $En_{46}Wo_{12}$ (Table 5).

Subcalcic augite

Subcalcic augite shows a similar range in composition (in terms of XFe) as orthopyroxene. The extreme values are $En_{50}Wo_{41}$ and $En_{34}Wo_{44}$. Here, the exsolution led to an incre-

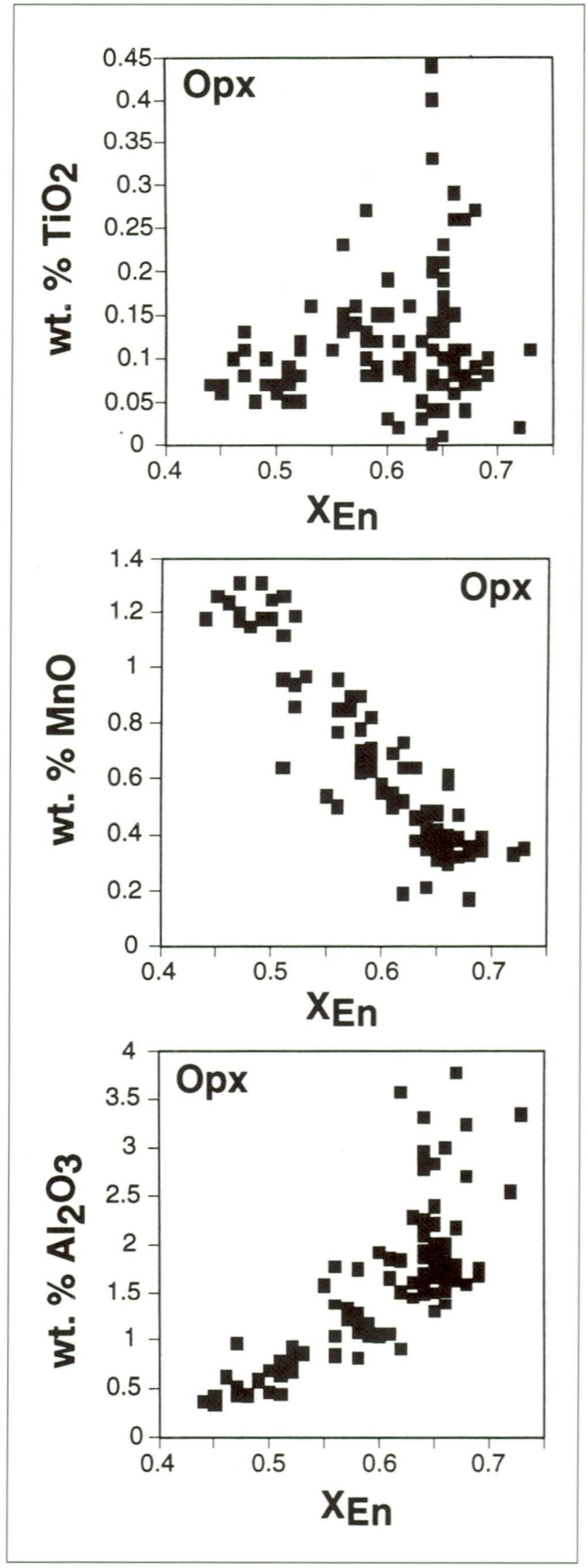

Fig. 12. Correlations between the En content of orthopyroxene (after the projection scheme of Lindsley 1983) from various Eidsfjord rocks and its TiO_2, MnO and Al_2O_3 contents. See text for discussion.

wt.%	1159-11 opx	1159-12 cpx	1159-13 pig	1096-3 opx	1096-2 cpx		1159-8 fsp	1159-9 fsp
SiO_2	51.20	52.44	51.15	52.68	52.24		61.80	62.57
TiO_2	0.08	0.21	0.06	0.33	0.28		0.00	0.00
Al_2O_3	0.66	1.35	1.02	1.94	2.54		23.12	22.29
FeO	28.10	10.73	27.55	20.59	11.95		0.13	0.04
MnO	1.19	0.44	1.03	0.36	0.26		0.01	0.00
MgO	17.33	12.43	15.83	22.53	15.44		0.01	0.01
CaO	0.61	22.20	3.87	1.79	17.27		4.57	3.73
Na_2O	0.03	0.36	0.07	0.05	0.36		5.76	4.85
K_2O	0.02	0.00	0.04	0.02	0.00		4.76	6.83
Total	99.23	100.19	100.66	100.34	100.40		100.18	100.32
Formula based on 4 cations and 6 oxygens (pyroxenes) or 5 cations (feldspars)								
Si	1.99	1.97	1.96	1.94	1.94		2.78	2.82
Al	0.03	0.06	0.05	0.08	0.11		1.22	1.18
Ti	0.00	0.01	0.00	0.01	0.01		0.00	0.00
Fe^{3+}	0.00	0.02	0.03	0.01	0.03		0.00	0.00
Mg	1.00	0.70	0.91	1.24	0.85		0.00	0.00
Fe^{2+}	0.91	0.32	0.85	0.62	0.35		0.00	0.00
Mn	0.04	0.01	0.03	0.01	0.01		0.00	0.00
Ca	0.03	0.89	0.16	0.07	0.69		0.22	0.18
Na	0.00	0.03	0.01	0.00	0.03		0.50	0.42
K	0.00	0.00	0.00	0.00	0.00		0.27	0.39
Sum	4.00	4.00	4.00	4.00	4.00		5.00	5.00
Pyroxene projection after Lindsley (1983)								
Wo	0.01	0.45	0.12	0.04	0.33	An	0.22	0.18
En	0.52	0.38	0.46	0.64	0.48	Ab	0.50	0.43
Fs	0.47	0.17	0.42	0.32	0.19	Or	0.27	0.39

Table 5. Representative electron microprobe analyses of mesoperthitic feldspar, orthopyroxene, clinopyroxene and inverted pigeonite in sample GM 1159 and of ortho- and clinopyroxene in sample GM 1096. All analyses were performed with a broad (c. 10 x 20 µm) electron beam.

ase in the Ca content of the clinopyroxene and hence the magmatic composition was significantly poorer in the Wo component. Only in a few cases did the finely developed exsolution lamellae allow for a reintegration of the original composition by broad-beam techniques on the microprobe. The lowest Wo component measured was $En_{48}Wo_{33}$ in sample GM 1096. The Al_2O_3 content varies between 1.2 and 4.95 wt.% with a wave-shaped correlation to X_{En} that is also observed in TiO_2 contents (Fig. 13). MnO, in contrast, shows a weak, but monotonous correlation to X_{En}. Fig. 10 plots all available clinopyroxene analyses into the pyroxene quadrilateral.

Feldspars

The feldspars show the strongest compositional variation in the Eidsfjord rocks. As Fig. 14 shows, gabbros contain K-poor plagioclase in the range An_{70}-An_{80}, the anorthosites show plagioclase between An_{40} and An_{60}, and the ferrodiorites and monzonites have strongly ternary feldspars with $An_{4\text{-}30}$ and $Or_{5\text{-}60}$ (with the monzonites having the highest Or contents). In the anorthosites, the Or contents analysed by the microprobe point measurements are significantly lower than the Or contents deduced from norm calculations from whole-rock analyses after the method detailed in Markl et al. (1998). Whereas in microprobe measurements, the Or content is consistently about 2 %, the normative feldspar compositions feature values up to 10 %. This is at least partly, and perhaps entirely caused by antiperthite exsolution of K-feldspar from the plagioclase which is commonly observed in most samples, but an influence of a residual, K-rich, interstitial liquid cannot be ruled out completely. However, no signs of the former presence of such an interstitial liquid were observed and the low Ba and Rb values of the anorthosites also do not support such an assumption.

The feldspars in the ferrodiorites are strongly exsolved. They were partly reconstructed via norm calculations as above, but in some cases the exsolutions were so fine that broad-beam microprobe techniques are believed to give reasonable reintegrated, magmatic feldspar compositions. The latter method was also used for the monzonites (see Fig. 14).

The FeO content is usually low but does reach 0.4 wt. % in some cases. Other elements were not measured.

Apatite

Apatite can cause problems during microprobe measurements due to the dependence of the measured halogen content on the angle between the c-axis of the crystal and the electron beam (Stormer at al. 1993). For the Eidsfjord rocks, this behaviour was confirmed (Fig. 15), because in the same sample, GM 1161, analyses of crystals which were cut perpendicular to the c-axis gave significantly higher Cl and lower F values than ones cut parallel

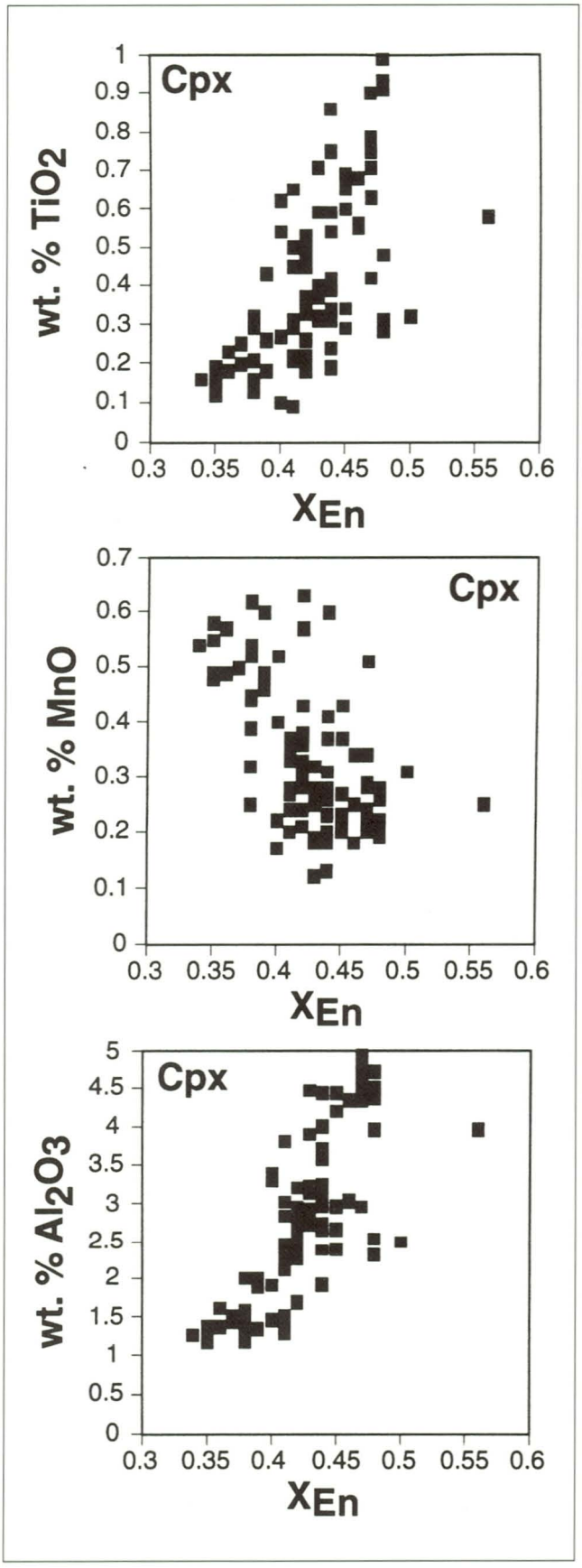

Fig. 13. Correlations between the En content of clinopyroxene (after the projection scheme of Lindsley 1983) from various Eidsfjord rocks and its TiO_2, MnO and Al_2O_3 contents. See text for discussion.

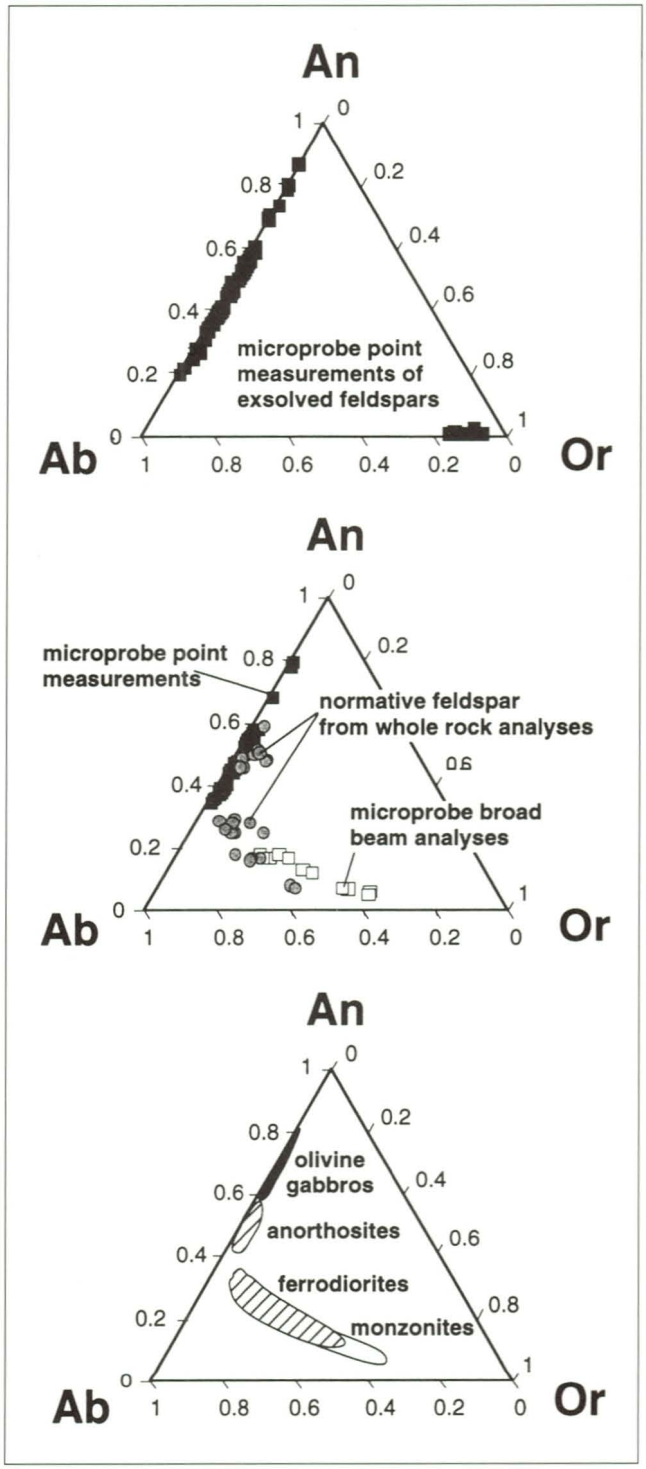

Fig. 14. Microprobe measurements and normative compositions of feldspars from the Eidsfjord rocks. Note the measurements of exsolved grains in the uppermost diagram in contrast to the broad-beam microprobe analyses and the normative compositions in the middle diagram. The lower diagram shows tentative fields for gabbros, anorthosites and gabbronorites, ferrodiorites and monzonitic rocks (including mangerites) in order to illustrate the evolution trend.

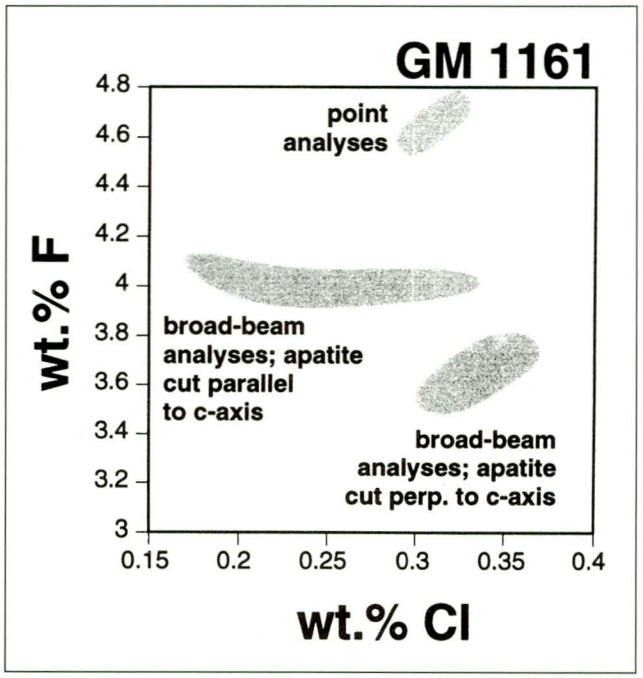

Fig. 15. Fluorine against chlorine (in wt. %) plot showing the difficulties involved in obtaining quantitative halogene measurements of apatite. The fields combine various measurements. All measurements were made on one thin-section. The results are clearly different depending on the orientation of the apatite grain (see also Stormer et al. 1993) and on the measurement conditions (i. e., if a focussed or a broad beam is used). See text for discussion.

to the c-axis. For Cl, this is the strongest effect that can cause erroneous measurements. For F, however, the effect of using a focused electron beam versus a ca. 10 µm-wide defocused beam is much more significant (Fig. 15): point analyses give by about 15 relative % higher F values than broad-beam analyses. These effects were also observed in the other samples that were investigated. Only broad-beam analyses were used and only the measurements from crystals that were cut parallel to their c-axis (i. e., elongate crystals in thin-section) for comparisons among samples or with the trends observed in other minerals. As shown in Fig. 16, this method considerably reduces the scatter in the data. This figure also illustrates the fact that apatites from monzonites, norites, ferrodiorites and anorthosites all lie on a continuous trend. At values higher than about 0.5 wt.% Cl, the trend of decreasing F with increasing Cl changes to increasing F and Cl. Most samples show very F-rich and relatively Cl-poor apatite, but in one sample (GM 1138), the Cl content in some crystals exceeds that of F. The total amount of halogen is so high that in many analyses no OH can be present and the halogens even exceed the one lattice site typically available for them. 1.2-1.3 halogen atoms per formula unit are not uncommon (Table 6) and only the low-Cl/low-F apatites of Fig. 16 can contain minor amounts (0.25 atoms per formula unit at the most) of OH.

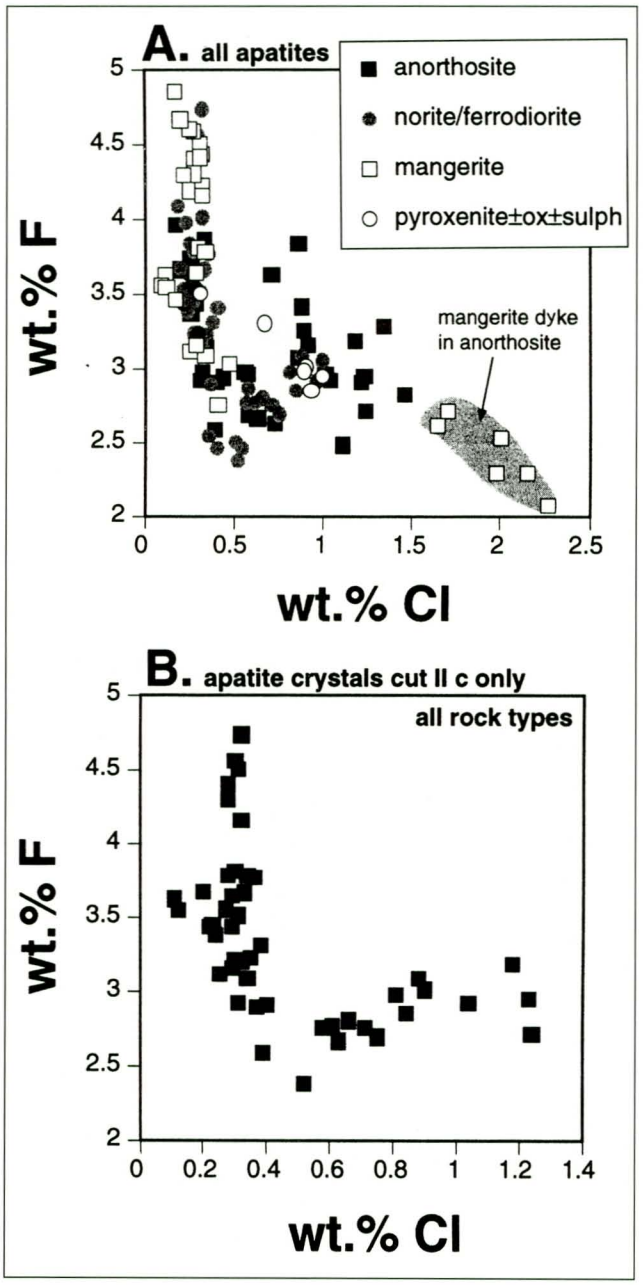

Fig. 16. Fluorine versus chlorine plot (in wt. %); (A) for all microprobe measurements of Eidsfjord apatites, and (B) for apatite crystals cut parallel to the c-axis only. The apatites come from all rock types encountered in the Eidsfjord anorthosite complex.

wt.%	1161 -12 ap	1159 -23 ap	1153 -13 ap	1152 -7 ap	1151 -9 ap	1150 -12 ap	1141 -9 ap	1140 -9 ap	1139 -15 ap	1132 -20 ap	1132 -25 ap	1131 -13 ap	1130 -13 ap
CaO	54.97	55.16	55.33	55.00	55.17	54.14	54.82	54.95	54.95	55.52	53.14	54.80	54.12
P_2O_5	42.48	42.63	42.95	42.77	42.47	42.02	41.83	43.06	42.83	43.08	39.16	41.83	41.87
Cl	0.31	0.12	0.35	0.34	0.31	0.88	0.30	0.32	0.34	1.24	2.15	1.23	0.58
F	3.52	3.54	3.22	3.08	3.50	3.09	3.81	4.15	3.78	2.71	2.29	2.95	2.75
Total corrected													
for F, Cl	99.72	99.93	100.42	99.82	99.91	98.63	99.09	100.67	100.25	101.12	95.29	99.28	98.03
Formula based on 8 cations and 12.5 oxygens													
Ca	4.95	4.95	4.93	4.93	4.96	4.94	4.99	4.91	4.92	4.94	5.09	4.99	4.95
P	3.02	3.02	3.03	3.03	3.02	3.03	3.01	3.04	3.03	3.03	2.96	3.01	3.02
Cl	0.04	0.02	0.05	0.05	0.04	0.13	0.04	0.05	0.05	0.17	0.33	0.18	0.08
F	0.93	0.94	0.85	0.82	0.93	0.83	1.02	1.09	1.00	0.71	0.65	0.79	0.74
Sum	7.97	7.97	7.96	7.96	7.98	7.96	7.99	7.94	7.95	7.96	8.05	7.99	7.97
900°C, 5 kbar													
f_{HCl}/f_{HF}	0.13	0.05	0.16	0.16	0.13	0.42	0.12	0.11	0.13	0.67	1.39	0.61	0.31
f_{H2O}/f_{HCl}	33.40	188.26	137.72	185.72	41.71	21.72	0.00	0.00	0.00	43.74	5.22	11.97	136.74
f_{H2O}/f_{HF}	4.28	9.20	21.95	30.43	5.42	9.16	0.00	0.00	0.00	29.46	7.23	7.35	42.71
1000°C, 5 kbar													
f_{HCl}/f_{HF}	0.10	0.04	0.12	0.12	0.10	0.32	0.09	0.09	0.10	0.51	1.05	0.47	0.24
f_{H2O}/f_{HCl}	19.22	108.33	79.25	106.87	24.00	12.50	0.00	0.00	0.00	25.17	3.00	6.89	78.69
f_{H2O}/f_{HF}	1.87	4.01	9.58	13.28	2.37	4.00	0.00	0.00	0.00	12.86	3.16	3.21	18.64

wt.%	1124 -12 ap	1120 -17 ap	1118 -9 ap	1109 -10 ap	1107 -7 ap	1105 -12 ap	1100 -9 ap	1091 -14 ap	1088 -9 ap	1087 -14 ap	1085 -15 ap	1082 -10 ap
CaO	54.93	54.97	55.20	54.98	54.08	54.69	55.66	54.22	54.93	54.64	55.88	54.71
P_2O_5	42.00	42.29	42.07	41.70	41.90	41.91	42.74	42.00	41.80	41.96	42.21	42.08
Cl	0.28	0.24	0.30	0.67	0.90	0.88	0.17	0.31	0.61	0.71	0.23	0.52
F	3.78	3.38	3.21	3.30	3.01	3.41	3.96	2.92	2.77	2.75	3.44	2.38
Total corrected												
for F, Cl	99.33	99.40	99.37	99.11	98.41	99.26	100.83	98.14	98.80	98.75	100.26	98.57
Formula based on 8 cations and 12.5 oxygens												
Ca	4.98	4.96	4.99	5.00	4.94	4.97	4.97	4.94	4.99	4.97	5.02	4.96
P	3.01	3.02	3.00	3.00	3.02	3.01	3.01	3.02	3.00	3.01	2.99	3.01
Cl	0.04	0.03	0.04	0.10	0.13	0.13	0.02	0.04	0.09	0.10	0.03	0.07
F	1.01	0.90	0.86	0.89	0.81	0.91	1.04	0.79	0.74	0.74	0.91	0.64
Sum	7.99	7.98	7.99	8.00	7.96	7.98	7.98	7.97	8.00	7.98	8.01	7.98
900°C, 5 kbar												
f_{HCl}/f_{HF}	0.11	0.10	0.14	0.30	0.44	0.38	0.06	0.15	0.32	0.38	0.10	0.32
f_{H2O}/f_{HCl}	0.00	127.27	152.83	11.65	29.79	0.00	0.00	255.81	129.29	103.77	112.91	253.36
f_{H2O}/f_{HF}	0.00	13.29	21.38	3.47	13.06	0.00	0.00	39.59	41.72	39.49	11.20	81.95
1000°C, 5 kbar												
f_{HCl}/f_{HF}	0.08	0.08	0.11	0.23	0.33	0.29	0.05	0.12	0.24	0.29	0.08	0.25
f_{H2O}/f_{HCl}	0.00	73.24	87.94	6.70	17.14	0.00	0.00	147.20	74.40	59.71	64.97	145.80
f_{H2O}/f_{HF}	0.00	5.80	9.33	1.51	5.70	0.00	0.00	17.28	18.21	17.24	4.89	35.77

Table 6. Selected electron microprobe analyses of apatite from samples from the Eidsfjord anorthosite complex and halogen acid/water fugacity ratios calculated therefrom. For discussion and explanations, see text. The reported measurements are only of crystals cut parallel to the c-axis.

Discussion

Estimates of intrinsic variables (P, T, aSiO2, fO2)

Intrinsic variables may be estimated with phase equilibria among the mafic silicate and Fe-Ti oxide phases using the QUIIF approach of Lindsley & Frost (1992) and Frost & Lindsley (1992) with the QUILF software of Andersen et al. (1993). This technique, however, requires knowledge about the magmatic phase compositions of at least some of the minerals (see e. g. Markl et al. 1998). This requirement is not generally fulfilled in plutonic rocks because of the exsolution and oxidation features in pyroxenes and in Fe-Ti oxides, and due to later Fe-Mg diffusive reequilibration during cooling. In the present case, exsolution features that could not

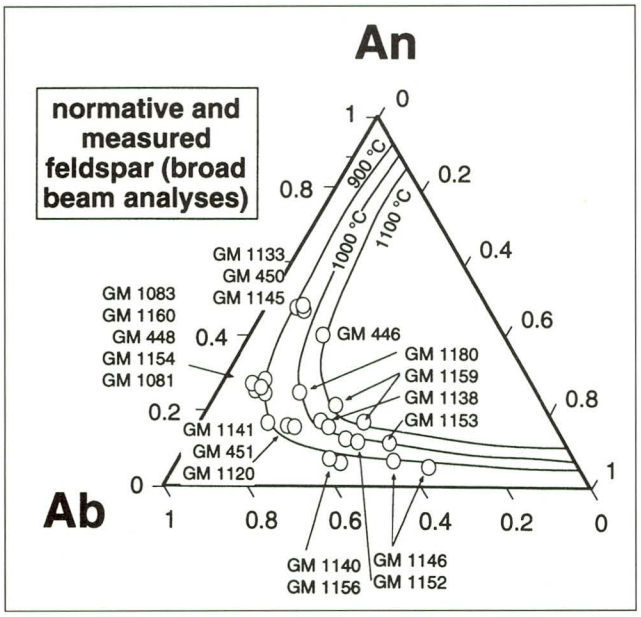

Fig. 17. Normative feldspar compositions and broad-beam electron microprobe analyses of feldspars from various rock types in the Eidsfjord anorthosite plotted onto the temperature-dependent feldspar solvus of Fuhrman & Lindsley (1988). Most samples indicate minimum temperatures in excess of 1000 °C, but see detailed discussion in the text.

be reintegrated prevented application of the QUIIF technique in all but two samples (GM 1096, GM 1159).

Another important constraint on the temperatures of crystallization is given by the presence of the strongly ternary feldspars in the ferrodiorites, some anorthosites and in the monzonites. Fig. 17 shows the calculated and measured (see above for explanation) feldspar compositions plotted on the temperature-dependent feldspar solvus as determined by Fuhrman & Lindsley (1988). The presence of a single ternary feldspar provides a minimum temperature constraint. The combination of feldspar thermometry with the QUIIF method could be used to deduce information on P, T and fo_2 values during crystallization of the Eidsfjord rocks (for detailed explanation of the technique see Markl et al. 1998).

Feldspar thermometry revealed minimum temperatures between 900° and 1100°C for the anorthositic, ferrodioritic and monzonitic rocks from Eidsfjord (Fig. 17). In particular, the highest temperatures are indicated by the feldspar composition in sample GM 1159 (Table 5). This temperature is interpreted to be the minimum liquidus temperature, while the equilibria among the mafic silicates give the solidus conditions (reequilibration with the last melt). Accordingly, it seems reasonable to assume that sample GM 1159 crystallized in the temperature interval 1200 to 1000°C. For this temperature interval, the pressure of crystallization could be calculated with QUILF using the measured composition of the pigeonite ($En_{46}Wo_{12}$) in the assemblage pigeonite+orthopyroxene. With this method, the pressure of intrusion was estimated to 5 ± 0.5 kbar. At the same time, fo_2 could be calculated at these temperatures and pressures because the assemblage contains two Fe-Ti oxide phases and quartz. For the temperatures as above and an SiO_2 activity of one (i. e. pure quartz at the P and T of interest), fo_2 was calculated to lie between 0.65 and -0.12 log units above or below the FMQ buffer.

In sample GM 1096, the assemblage Cpx+Opx allowed determination of the solidus temperature at a fixed pressure. It was assumed that the anorthosite (GM 1096) and the monzonite (GM 1159) crystallized at the same pressure. At 5 kbar, the Cpx and Opx compositions in GM 1096 indicate a temperature of 1115°C. The reaction

$$CaAl_2SiO_6 + SiO_2 = CaAl_2Si_2O_8$$

allows determination of the silica activity in rocks with coexisting plagioclase and clinopyroxene (see Markl et al. 1998). At the pressure and temperature of interest and with suitable solution models applied to the measured mineral compositions (Wood 1979, for the CATS-component in clinopyroxene, Fuhrman & Lindsley 1988, for the anorthite component in plagioclase), this reaction indicates SiO_2 activities on the order of 0.45-0.54 (Fig. 18). These results are at slight variance with the results of Markl et al. (1998) who estimated silica activities based on QUIIF equilibria to be greater than 0.64 for sample GM 452 from the Eidsfjord anorthosite, while their pressure and temperature estimates closely agree with the estimates presented here. The reason for the discrepancy is unclear because both samples are anorthosites s.s., but they may reflect small differences in melt evolution between both samples. In summary, however, it can be stated that the monzonites, as well as the anorthosites, show liquidus temperatures above 1100°C and solidus temperatures above 1000 °C with oxygen fugacities in the range FMQ ± 0.5. The monzonite intruded to mid-crustal levels at a depth of about 17 km.

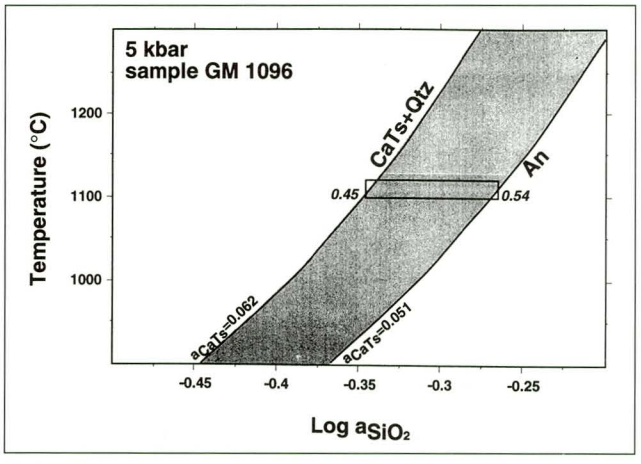

Fig. 18. Temperature vs. log $^{a}_{SiO2}$ diagram. The reaction Ca-tschermakite + SiO_2 = anorthite was calculated for the range of mineral compositions observed in sample GM 1096 and for a constant pressure of 5 kbar. At 1100 °C, the reaction 'band' indicates silica activities between 0.45 and 0.54 for this sample.

Preliminary estimates on fluid composition and evolution during the magmatic stage

Anorthosites and related rocks show an anhydrous mineralogy involving pyroxenes, Fe-Ti oxides, olivine and feldspars. The occurrence of sparse late-magmatic amphibole or biotite in some monzonitic rocks allows in some cases for the calculation of HF, HCl and H_2O fugacities (e. g. Kolker & Lindsley 1989, Markl et al. 1998, Markl & Piazolo, 1998). These generally lie considerably below lithostatic pressure and in the order of 0.01-1 bars for HF, 1-300 bars for HCl and 10-2000 bars for H_2O. In the anorthosites and more mafic rocks, amphibole and biotite occur only as metamorphic overgrowths on the primary anhydrous minerals and, hence, the only possibility to deduce any information on the fluid composition is to use the apatite-fluid equilibria of Zhu & Sverjensky (1991). This method allows estimation of f_{HCl}/f_{HF}, f_{H2O}/f_{HF} and f_{H2O}/f_{HCl} ratios at a fixed pressure and temperature. However, the experiments of Zhu & Sverjensky (1991) have been performed at 1 and 2 kbar only and extrapolation to 5 kbar may not be valid. Furthermore, the apatite analyses of the present study indicate significant involvement of species like CO_3^{2-} not considered in the work of Zhu & Sverjensky (1991). Hence, with this caveat in mind, the following calculated values are only broad, preliminary approximations: at 1000 °C, H_2O/HF fugacity ratios range between zero and 36 and HCl/HF fugacity ratios between zero and 0.6, in one sample (GM 1132) up to 1.2. At 900 °C, those values are approximately doubled. Wheras the calculated HCl values are in accordance with the values from the literature mentioned above, all calculated HF values are significantly different in that they show extremely high HF/H_2O ratios.

In Fig. 19 the halogen content of apatite is plotted against the magmatic An content of the feldspar and against the En content of the orthopyroxene in the same sample. Weak trends indicate decreasing Cl and increasing F contents in the apatite with more Fe-rich pyroxene and Ca-poor feldspar compositions, hence with advancing fractionation. These results indicate the very low water content of the early, more primitive magmas and the increasing F content in the melt during fractionation. The decrease in Cl in apatite may not reflect the content of Cl in the melt but rather the evolution of F/Cl ratios in the melt, which progressively become higher. As partitioning of F into apatite is highly favoured over the incorporation of Cl, the latter can decrease in apatite even though it may actually increase in the coexisting melt.

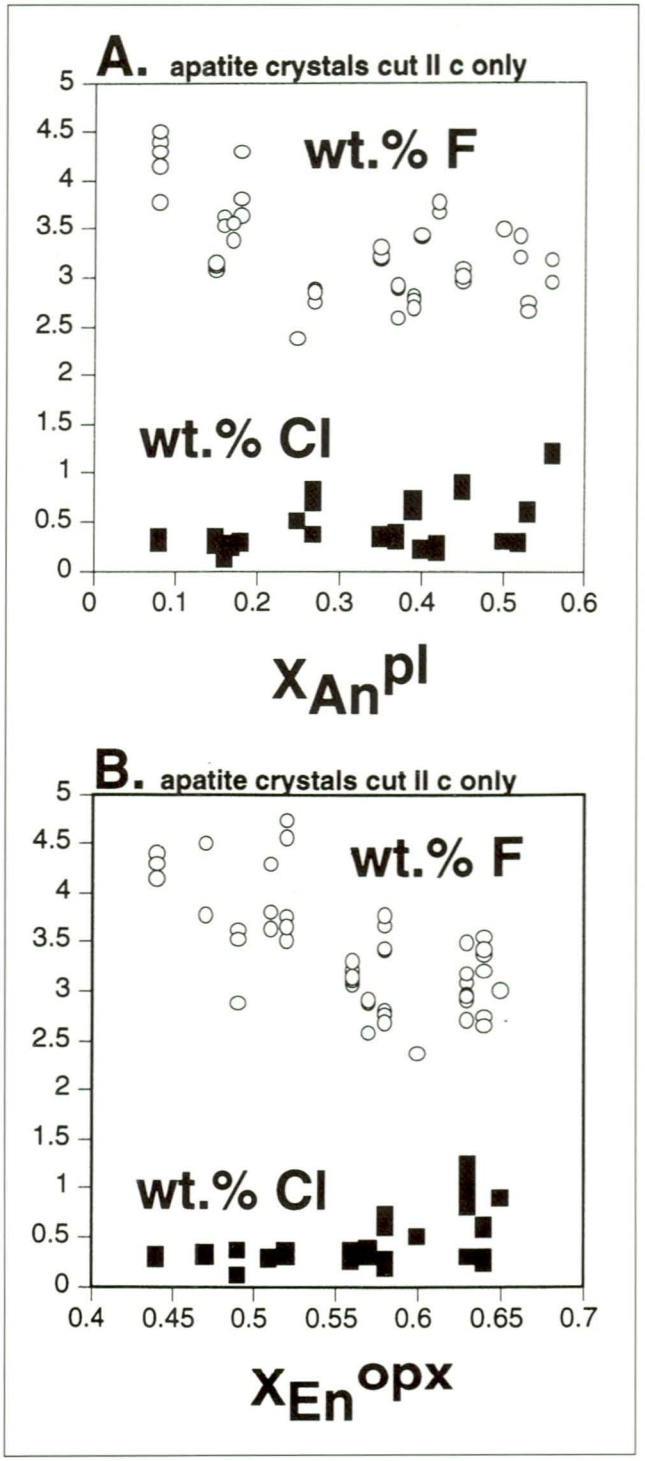

Fig. 19. Covariation of apatite halogen content (wt. % F and Cl, respectively) with the An content of feldspar (A) and with the En content of Opx (B) from the same sample.

The connection between whole-rock and mineral chemistry

In some previous sections, both whole-rock and mineral chemical data were presented that indicate a fractionation trend from primitive gabbroic via anorthositic and ferrodioritic possibly to the monzonitic rocks. The question of the effect of cumulus processes on whole-rock analyses is always a matter of concern in non-glassy rocks. The samples used are all fine-grained and are interpreted to reflect liquid compositions based on their aphyric textures. This is supported by the available REE analysis. As another support and in order to tie the ob-

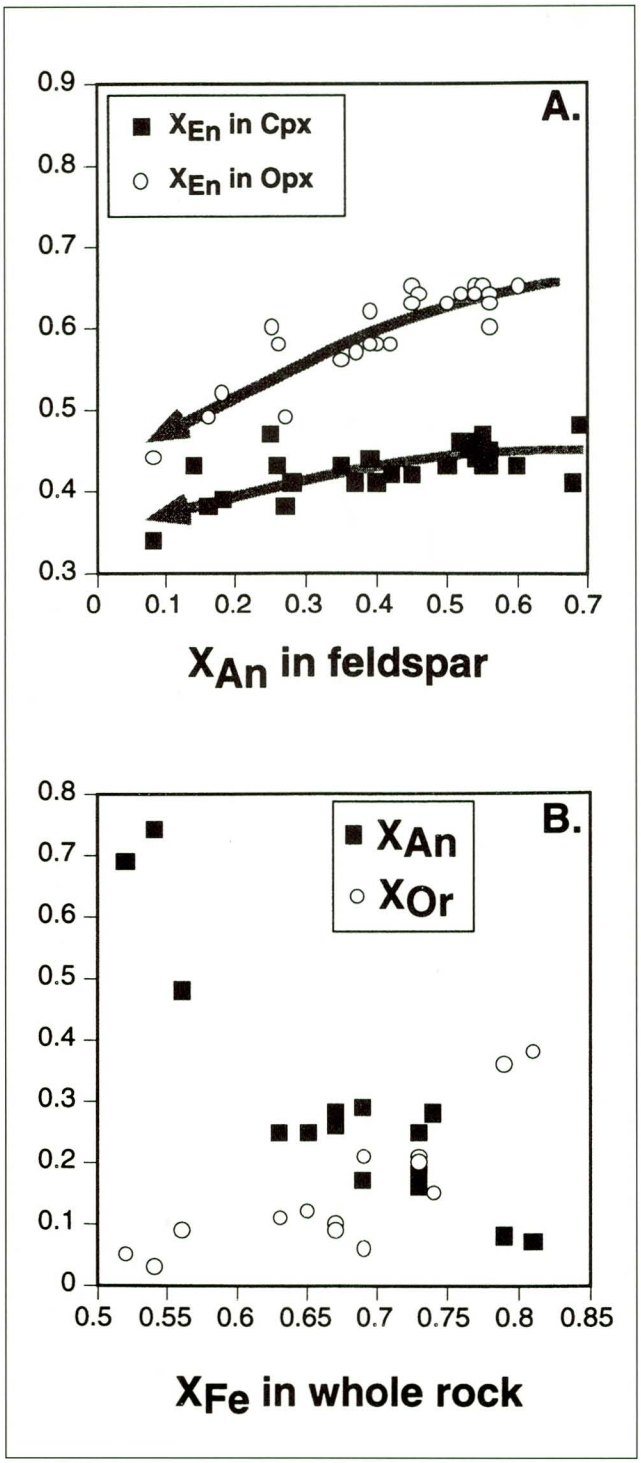

Fig. 20. Covariation of the En content of orthopyroxene and clinopyroxene with the An content of feldspar from the same sample (A) and of the An and Or content of the feldspar with X_{Fe} of the whole rock (B).

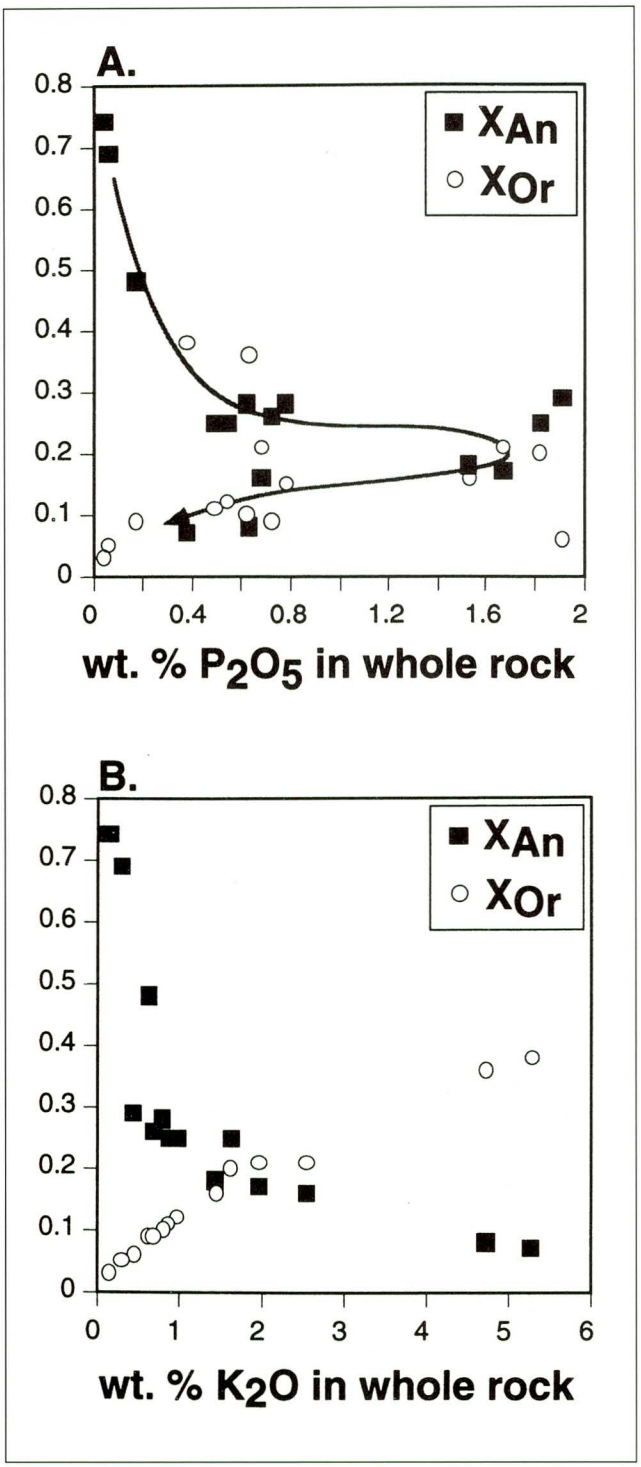

Fig. 21. Covariation of the An and Or content of the feldspar with P_2O_5 content of the whole rock (A) and with K_2O content of the whole rock (B).

served mineral to the whole-rock compositions, Fig. 20 plots the En content of pyroxenes and the An and Or content of feldspars against the whole rock X_{Fe} value for the same sample. It is obvious that the trends in mineral and in whole-rock analyses generally agree well. The good agreement between mineral and whole-rock trends is also indicated by plots of magmatic feldspar composition against wt. % P_2O_5 and K_2O in whole rock (Fig. 21). These have the same shapes as the plots against X_{Fe} in Fig. 7 including the extreme phosphorus enrichment in the evolved ferrodiorites, which plot at X_{An} values of about 0.15-0.3 in Fig. 21 A plot of pyroxene composition against whole-rock S and K_2O contents shows for K_2O again the larger scatter for clinopyroxene, but a

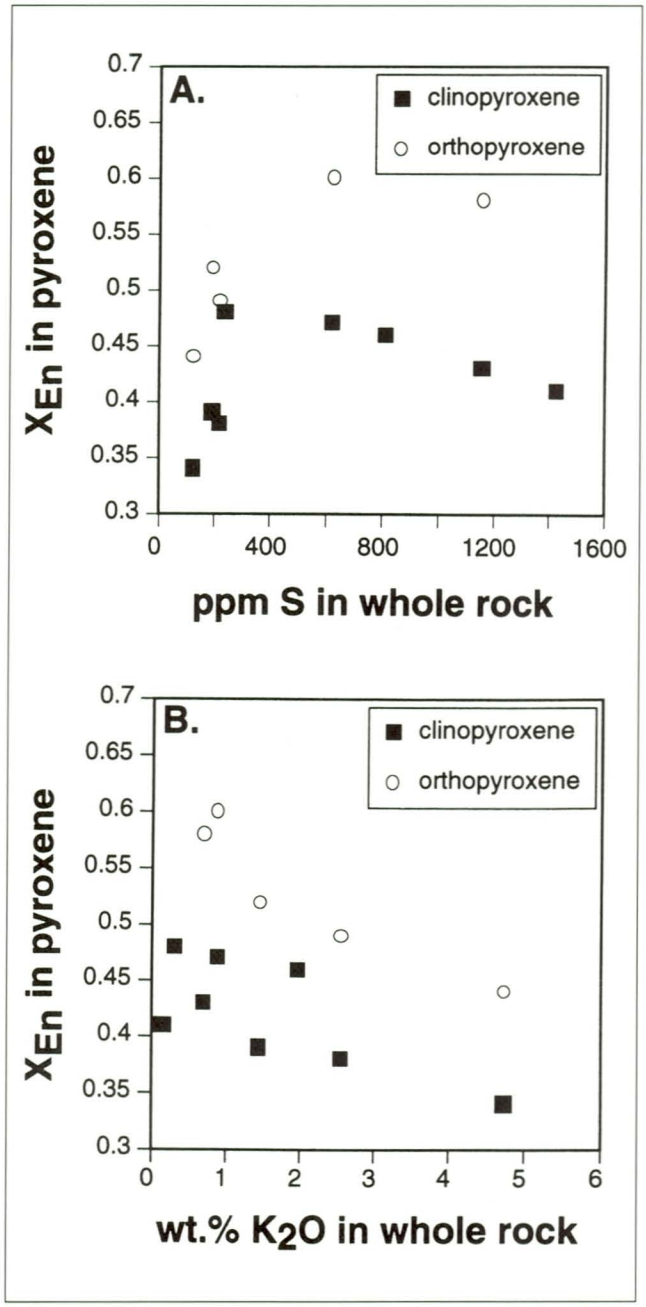

Fig. 22. Covariation of the En content of orthopyroxene and clinopyroxene with the S content of the whole rock (A) and with K_2O content of the whole rock (B).

good agreement between the mineral and whole-rock trends (Fig. 22). Interestingly, the plot against S indicates a well-defined relationship between the S, i. e. the sulphide content of a rock and the En component in the pyroxenes; while at low S contents, X_{En} increases with S, this trend is reversed at higher S contents (at least for clinopyroxene; for orthopyroxene, this trend is based on very few analyses). While it is expected that higher S concentrations in the melt favour the En component in Opx with which the trend at low S whole-rock contents is in agreement, the reason for the trend at high S contents is unclear.

Summary and conclusions

A continuous fractionation trend from gabbros to ferrodiorites and monzonites

The whole-rock geochemical and the mineral chemistry data record a trend in the Eidsfjord samples that starts at rocks with low X_{Fe} values, high Al_2O_3 and CaO and low K_2O, and which leads to extreme enrichment of FeO^{tot}, TiO_2 and P_2O_5 at X_{Fe} values around 0.8 and further on to rocks with high SiO_2 and K_2O and low CaO values at even higher X_{Fe}. As the compositions of feldspars and pyroxenes show increasingly evolved compositions with higher X_{Fe} values in the whole rock, this trend can be regarded as a fractionation trend. The trace element whole-rock data are in agreement with this interpretation as most of them show the expected behaviour (e. g. Ni, Cr, Co decrease with increasing X_{Fe}, Rb and Ba increase).

The trend from ferrodioritic to monzonitic rocks may be tentatively explained either by further fractionation (possibly combined with assimilation processes) or by the involvement of completely independent, e. g. anatectic, melts. The isotopic data on Lofoten rocks of Wade (1985), presented and interpreted by Markl and Frost (submitted), indicate that the first possibility is the more likely one for the Lofoten rocks. This assumption of a continuous fractionation trend, however, will be in question as long as a detailed isotopic study of the Eidsfjord rocks is lacking.

As a test for the feasability of the fractionation process to produce the observed succession of rocks from gabbros to ferrodiorites and the observed mineral compositions, calculations were performed using the MELTS program of Ghiorso et al. (1994). Fig. 23 shows the results for isobaric fractionation at 5 kbar during cooling from the liquidus (calculated to be ca. 1350°C according to the MELTS software) for sample GM 1127 under fo_2 conditions buffered by FMQ. Sample GM 1127, a fine-grained gabbro, was chosen for this calculation as it reflects the least evolved composition at Eidsfjord in terms of X_{Fe}. The calculated fractionation trends for major and minor elements agree very well with the ones exhibited by the whole-rock analyses of Fig. 7 and the sequence of fractionating minerals (spinel *s. l.*-olivine-clinopyroxene-plagioclase-orthopyroxene). The fractionation interval shown represents solidification of 90 % of the starting liquid. Further calculations yield unreasonable melt compositions with extreme Na_2O contents of >10 wt.%, and are therefore not reported here. The effects of assimilation were not taken into account as the results indicate that this process is of possible importance only for the last 10% of melt or so, hence the monzonitic rocks, which could not be modelled with MELTS anyway.

The calculated liquid evolution even reflects the extreme Fe-and Ti-enriched ferrodioritic rocks at about 70 % solidification and the relatively constant SiO_2 content of the melts over the first 70-80 % of fractionation. The feldspar compositions calculated to be in equilibrium with the liquid at tem-

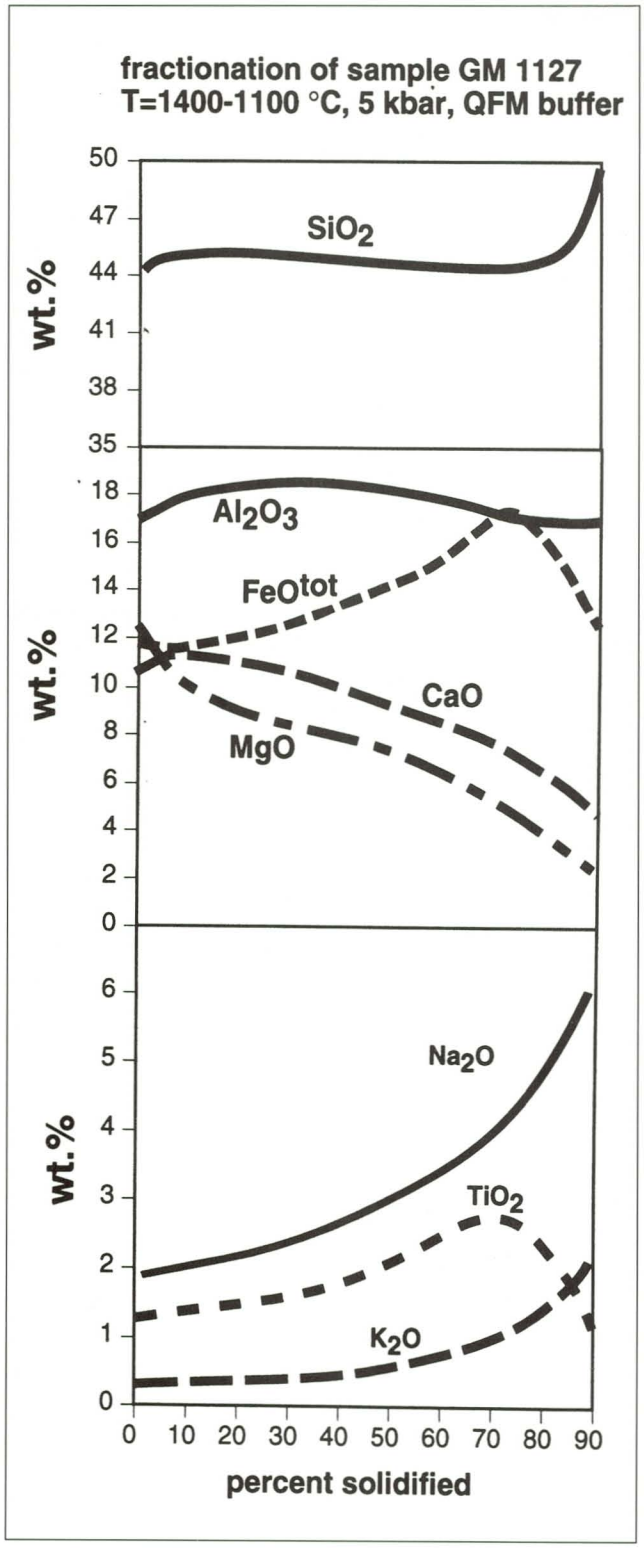

Fig. 23. Calculated liquid evolution lines in terms of wt.% of the major oxides against the percentage of the solidified liquid. These evolution lines are calculated for sample GM 1127 with the MELTS program of Ghiorso et al. (1994) for a temperature interval of 1400-1100 °C at 5 kbar and with an oxygen fugacity corresponding to that of the quartz-fayalite-magnetite (QFM) buffer. Sample GM 1127 is the most primitive sample found in the Eidsfjord anorthosite complex (in terms of $X_{Fe}^{whole\ rock}$). Note the strong similarities between these liquid evolution lines and the trends of the data shown in Fig. 8.

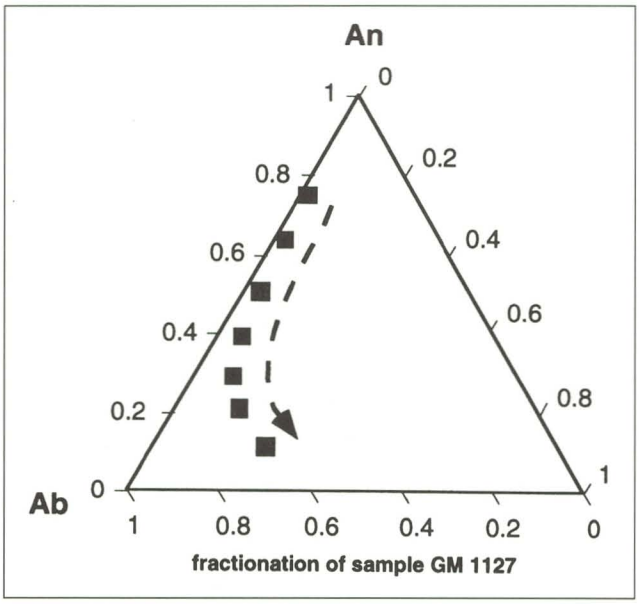

Fig. 24. Calculated feldspar compositions for the liquid evolution in Fig. 23. Note the similarity of the trend shown to the trend exhibited by the measured feldspar compositions in Figs. 14 and 17.

peratures between 1200 and 900 °C (Fig. 24) agree very well with the trend observed in the Eidsfjord rocks starting at $An_{75}Or_2$ and evolving towards strongly ternary alkali feldspars. The agreement between the observed trends of whole-rock and mineral analyses and the calculated ones is a strong support for the interpretation that a continuous fractionation from gabbroic to ferrodioritic rocks exists. The continuation to monzonitic rocks is neither supported nor disproved by the melt calculations. The results between 80 and 90% solidification, however, show increasing K_2O and SiO_2 and are therefore suggestive of a trend towards monzonitic compositions.

Synthesis of field observations and geochemical data

As the geochemical data indicate a fractionation trend in which the anorthosite forms at an intermediate stage between gabbros and ferrodiorites, it is expected that mafic rocks occur which are both younger and older than the anorthosite. Although some field observations indicate that the anorthosites are older than most of the more mafic rocks, especially the ferrodiorites, the contacts in some places at least support a contemporaneous formation of anorthosites and mafic rocks. In some places, the relationships are equivocal and hence the field observations are not in conflict with the geochemical data. The geochemically most evolved monzonitic rocks are clearly younger than the rest of the complex and here the data are in perfect agreement with the observations.

Volumetrically, the Eidsfjord anorthosite complex comprises about the same volume of leuconoritic to noritic rocks as true anorthosites while the ferrodiorites are clearly less common. The amount of monzonites cannot be estimated reliably, because it is not clear if any of the more or less de-

formed and retrogressed monzonites to the northwest and to the south of the anorthosite are genetically related to the Eidsfjord anorthosite.

The finding of a continuous fractionation trend from gabbros to ferrodiorites and possibly monzonitic rocks in the relatively small Eidsfjord anorthosite complex may render this anorthosite a good example of the processes responsible for anorthosite formation. As mentioned earlier, the question of parental magmas for anorthosite and their geochemical evolution is still under debate (e. g. Emslie 1989, Olson & Morse 1990, Mitchell et al. 1995, 1996, Scoates et al. 1996, Vander Auwera et al. 1998, Markl & Frost in press,), but it has been arrowed down to a Skaergaard-type fractionation trend of tholeiitic basalt to ferrodiorites with extreme Fe- and P-enrichment and finally to rocks of broadly granitic composition (e. g. Mitchell et al. 1995, 1996, Scoates et al. 1996, Markl & Frost in press). This fractionation trend in the case of the Eidsfjord anorthosite, is completely recorded within a single, relatively small complex. With this knowledge about the type of melt and the type of fractionation involved in the genesis of anorthosites at hand, our understanding of the other enigmatic features of anorthosites may be rendered less difficult.

Acknowledgements

I am grateful to K. Bucher, Universtät Freiburg, who introduced me to the Lofoten rocks, to B. R. Frost, University of Wyoming, who provided a lot of suggestions to think about, and especially to S. Piazolo, Universität Mainz, for her assistance during the fieldwork and for helpful comments on an earlier version of the manuscript. The thorough and constructive reviews of L. Ashwal and J.-C. Duchesne and comments by E. Tveten are very much appreciated. The help of the staff of the Institut für Mineralogie, Petrologie und Geochemie and of H. Gräf, Institut für Geologie, is gratefully acknowledged. This work was funded by grants Bu 843/3-1, 3-2 and 3-3 from the Deutsche Forschungsgemeinschaft.

References

Andersen, D. J., Lindsley, D. H. & Davidson, P. M. 1993: QUILF: a pascal program to assess equilibria among Fe-Mg-Mn-Ti oxides, pyroxenes, olivine, and quartz. *Computers & Geosciences 19*, 1333-1350.

Ashwal, L. D. 1993: *Anorthosites*. Springer-Verlag Berlin, 422 pp.

Deer, W. A., Howie, R. A. & Zussman, J. 1992: *An introduction to the rock-forming minerals*. Longman Scientific and Technical, Harlow (Essex) 2nd edition 696 pp.

Duchesne, J.-C. 1984: Massif anorthosites: another partisan review. In: Brown, W. L. (ed.). *Feldspars and Feldspathoids*. D. Reidel Publishing Company Dordrecht, p. 411-433.

Duchesne, J. - C. & Wilmart, E. 1997: Igneous charnockites and related rocks from the Bjerkreim-Sokndal Layered Intrusion (Southwest Norway): a jotunite (hypersthene monzodiorite)-derived A-type granitoid suite. *Journal of Petrology 38*, 337-369.

Emslie, R. F. 1975: Pyroxene megacrysts from anorthositic rocks: new clues to the source and evolution of the parent magmas. *Canadian Mineralogist 13*, 138-145.

Emslie, R. F. 1978: Anorthosite massifs, rapakivi granites, and late Proterozoic rifting of North America. *Precambrian Research 7*, 61-98.

Emslie, R. F. 1989: Geology and petrology of the Harp Lake Complex, central Labrador: an example of Elsonian magmatism. *Geological Survey of Canada Bulletin 293*, 1-136.

Emslie, R. F. & Hunt, P. A. 1990: Ages and petrogenetic significance of igneous mangerite-charnockite suites associated with massif anorthosites, Grenville province. *Journal of Geology 98*, 213-231.

Emslie, R. 1991: Granitoids of rapakivi granite-anorthosite and related associations. *Precambrian Research 51*, 173-192.

Fram, M. S. & Longhi, J. 1992: Phase equilibria of dikes associated with Proterozoic anorthosite complexes. *American Mineralogist 77*, 605-616.

Frost, B. R. & Lindsley, D. H. 1992: Equilibria among Fe-Ti oxides, pyroxenes, olivine, and quartz: Part II. Application. *American Mineralogist 77*, 1004-1020.

Fuhrman, M. L., Frost, B. R. & Lindsley, D. H. 1988: Crystallization conditions of the Sybille monzosyenite, Laramie anorthosite complex, Wyoming. *Journal of Petrology 29*, 699-729.

Fuhrman, M. & Lindsley, D. 1988: Ternary-feldspar modeling and thermometry. *American Mineralogist 73*, 201-215.

Ghiorso, M. S., Hirschmann, M. M. & Sack, R. O. 1994: MELTS: Software for thermodynamic modeling of magmatic systems. *EOS 75*, 571.

Griffin, W. L., Taylor, P. N., Hakkinen, J. W., Heier, K. S., Iden, I. K., Krogh, E. J., Malm, O., Olsen, K. I., Ormaasen, D. E. & Tveten, E. 1978: Archean and Proterozoic crustal evolution in Lofoten-Vesterålen, N Norway. *Journal of the Geological Society of London 135*, 629-647.

Hames, W. E. & Andresen, A. 1996: The timing of Paleozoic orogeny and extension in the continental shelf of northcentral Norway as indicated by laser $^{40}Ar/^{39}Ar$ muscovite dating. *Geology 24*, 1005-1008.

Heier, K. S. 1960: Petrology and Geochemistry of High-grade Metamorphic and Igneous Rocks on Langøy, Northern Norway. *Norges geologiske undersøkelse Bulletin 207*, 1-246.

Johnson, J. W., Oelkers, E. H. & Helgeson, H. C. 1992: SUPCRT92: A software package for calculating the standard molal thermodynamic properties of minerals, gases, aqueous species, and reactions from 1 to 5000 bars and 0 to 1000°C. *Computers & Geosciences 18*, 899-947.

Kolker, A. & Lindsley, D. H. 1989: Geochemical evolution of the Maloin Ranch pluton, Laramie anorthosite complex, Wyoming: petrology and mixing relations. *American Mineralogist 74*, 307-324.

Kolker, A., Lindsley, D. H. & Hanson, G. N. 1990: Geochemical evolution of the Maloin Ranch pluton, Laramie Anorthosite Complex, Wyoming: trace elements and petrogenetic models. *American Mineralogist 75*, 572-588.

Krogh, E. J. 1977: Origin and metamorphism of iron formations and associated rocks, Lofoten-Vesterålen, N. Norway. I. The Vestpolltind Fe-Mn deposit. *Lithos 10*, 243-255.

Lafrance, B., John, B. E. & Scoates, J. S. 1996: Syn-emplacement recrystallization and deformation microstructures in the Poe Mountain anorthosite, Wyoming. *Contributions to Mineralogy and Petrology 122*, 431-440.

Lindsley, D. H. 1983: Pyroxene thermometry. *American Mineralogy 68*, 477-493.

Lindsley, D. H. & Frost, B. R. 1992: Equlibria among Fe-Ti oxides, pyroxenes, olivine, and quartz: Part I. Theory. *American Mineralogist 77*, 987-1003.

Longhi, J., Fram, M. S., Vander Auwera, J. & Montieth, J. N. 1993: Pressure effects, kinetics, and rheology of anorthositic and related magmas. *American Mineralogist 78*, 1016-1030.

Malm, O. & Ormaasen, D. E. 1978: Mangerite-charnockite Intrusives in the Lofoten-Vesterålen Area, North Norway: Petrography, Chemistry and Petrology. *Norges geologiske undersøkelse Bulletin 338*, 83-114.

Markl, G. & Bucher, K. 1997: Proterozoic eclogites from the Lofoten Islands, N. Norway. *Lithos 42*, 15-35.

Markl, G., Frost, B. R. & Bucher, K. 1998: The origin of anorthosites and related rocks from the Lofoten Islands, Northern Norway: I. Field relations and estimation of intrinsic variables. *Journal of Petrology, 39*, 1425-1452.

Markl, G. & Frost, B. R. 1998: The origin of anorthosites and related rocks from the Lofoten Islands, Northern Norway: II. Modelling of parental melts for anorthosites. *Journal of Petrology 39*, 1425-1452.

Markl, G. & Frost, B. R. submitted: The origin of anorthosites and related rocks from the Lofoten Islands, Northern Norway: III. Isotope geochemistry and constraints on a liquid line of descent for mangerites. *Journal of Petrology*

Markl, G. & Piazolo, S. 1998: Halogen-bearing minerals in syenites and high-grade marbles of Dronning Maud Land, Antarctica: monitors of fluid compositional changes during late-magmatic fluid-rock interaction processes. *Contributions to Mineralogy and Petrology, 132*, 246-268.

Mitchell, J. N., Scoates, J. S. & Frost, C. D. 1995: High-Al gabbros in the Laramie Anorthosite Complex, Wyoming: implications for the composition of melts parental to Proterozoic anorthosite. *Contributions to Mineralogy and Petrology 119*, 166-180.

Mitchell, J. N., Scoates, J. S., Frost, C. D. & Kolker, A. 1996: The geochemical evolution of anorthosite residual magmas in the Laramie Anorthosite Complex, Wyoming. *Journal of Petrology 37*, 637-660.

Morse, S. A. 1982: A partisan review of Proterozoic anorthosites. *American Mineralogist 67*, 1087-1100.

Olsen, K. I. 1978: *Metamorphic petrology and fluid-inclusion studies of granulites and amphibolite-facies gneisses on Langøy and W Hinnøy, Vesterålen, N Norway*. Unpubl. Cand. Real. thesis, Univ. of Oslo, 214 pp.

Olson, K. & Morse, S. A. 1990: Regional Al-Fe mafic magmas associated with anorthosite bearing terranes. *Nature 344*, 760-762.

Pouchou, J. L. & Pichior, F. 1984: A new model for quantitative analysis. I. Application to the analysis of homogeneous samples. *La Recherche Aérospatiale 3*, 13-38.

Pouchou, J. L. & Pichior, F. 1985: 'PAP' f(rZ) procedure for improved quantitative analysis. *Microbeam Analysis 13*, 104-106.

Priesemann, F.-D. 1982: *Geologische Kartierung der gabbroiden Eidet-Hovden Intrusion, Vesteraalen, Nord-Norwegen sowie lagerstaettenkundliche und geochemische Bearbeitung der mit ihr verknuepften Titanomagnetit-Vererzungen.* Unpubl. Ph.D. thesis University of Clausthal, 282 pp.

Scoates, J. S., Frost, C. D., Mitchell, J. N., Lindsley, D. H. & Frost, B. R. 1996: Residual liquid origin for a monzonitic intrusion in a mid-proterozoic anorthosite complex: the Sybille intrusion, Laramie anorthosite complex, Wyoming. *Geological Society of America Bulletin 108*, 1357-1371.

Stormer, J. C., Pierson, M. L. & Tacker, R. C. 1993: Variation of F and Cl X-ray intensity due to anisotropic diffusion in apatite during electron microprobe analysis. *American Mineralogist 78*, 641-648.

Tveten, E. 1978: Beskrivelse til geologisk kart over Norge - 1:250 000, Svolvær. Norges geologiske undersøkelse, Trondheim.

Vander Auwera, J., Longhi, J. & Duchesne, J.-C. 1998: A liquid line of descent of the jotunite (hypersthene monzodiorite) suite. *Journal of Petrology 39*, 439-468.

Wade, S. J. R. 1985: *Radiogenic isotope studies of crust-forming processes in the Lofoten-Vesterålen Province of North Norway*. Unpubl. Ph.D. Thesis, University of Oxford, 285 pp.

Wiebe, R. A. 1992: Proterozoic anorthosite complexes. In: Condie, K. C. (ed.). *Proterozoic crustal evolution*. Elsevier, Amsterdam, 251-261.

Wood, B. J. 1979: Activity-composition relationships in Ca(Mg,Fe)Si2O6-CaAl2SiO6 clinopyroxene solid solution. *American Journal of Science 279*, 854-875.

Zhu, C. & Sverjensky, D. A. 1991: Partitioning of F-Cl-OH between minerals and hydrothermal fluids. *Geochimica et Cosmochimica Acta 55*, 1837-1858.

Manuscript received February 1998; revised manuscript accepted June 1998.